AMERICAN SOCIETY FOR MICROBIOLOGY | Journal of Virology®

VIRUS-CELL INTERACTIONS

HIV-1 Vpu Downmodulates ICAM-1 Expression, Resulting in Decreased Killing of Infected CD4$^+$ T Cells by NK Cells

Scott M. Sugden,[a] Tram N. Q. Pham,[a] Éric A. Cohen[a,b]

Laboratory of Human Retrovirology, Institut de Recherches Cliniques de Montréal (IRCM), Montreal, Quebec, Canada[a]; Department of Microbiology, Infectiology and Immunology, Université de Montréal, Montréal, Québec, Canada[b]

ABSTRACT HIV-1 Vpu is known to alter the expression of numerous cell surface molecules. Given the ever-increasing list of Vpu targets identified to date, we undertook a proteomic screen to discover novel cell membrane proteins modulated by this viral protein. Plasma membrane proteome isolates from Vpu-inducible T cells were subjected to *s*table isotope labeling of amino acids in cell culture (SILAC)-based mass spectrometry analysis, and putative targets were validated by infection of primary CD4$^+$ T cells. We report here that while intercellular adhesion molecule 1 (ICAM-1) and ICAM-3 are upregulated by HIV-1 infection, expression of Vpu offsets this increase by downregulating these molecules from the cell surface. Specifically, we show that Vpu is sufficient to downregulate and deplete ICAM-1 in a manner requiring the Vpu transmembrane domain and a dual-serine (S52/S56) motif necessary for recruitment of the beta-transducin repeat-containing E3 ubiquitin protein ligase (β-TrCP) component of the Skp, Cullin, F-box (SCF$^{\beta\text{-TrCP}}$) E3 ubiquitin ligase. Vpu interacts with ICAM-1 to induce its proteasomal degradation. Interestingly, the E3 ubiquitin ligase component β-TrCP-1 is dispensable for ICAM-1 surface downregulation yet is necessary for ICAM-1 degradation. Functionally, Vpu-mediated ICAM-1 downregulation lowers packaging of this adhesion molecule into virions, resulting in decreased infectivity. Importantly, while Vpu-mediated downregulation of ICAM-3 has a limited effect on the conjugation of NK cells to HIV-1-infected CD4$^+$ T cells, downregulation of ICAM-1 by Vpu results in a reduced ability of NK cells to bind and kill infected T cells. Vpu-mediated ICAM-1 downregulation may therefore represent an evolutionary compromise in viral fitness by impeding the formation of cell-to-cell contacts between immune cells and infected T cells at the cost of decreased virion infectivity.

IMPORTANCE The major barrier to eradicating HIV-1 infection is the establishment of treatment-resistant reservoirs early in infection. Vpu-mediated ICAM-1 downregulation may contribute to the evasion of cell-mediated immunity during acute infection to promote viral dissemination and the development of viral reservoirs. By aiding the immune system to clear infection prior to the development of reservoirs, novel treatments designed to disrupt Vpu-mediated ICAM-1 downregulation may be beneficial during acute infection or as a prophylactic treatment.

KEYWORDS ICAM-1, NK cell-mediated killing, Vpu, human immunodeficiency virus, immune evasion, immunological synapse, viral infectivity

Received 16 December 2016 **Accepted** 26 January 2017

Accepted manuscript posted online 1 February 2017

Citation Sugden SM, Pham TNQ, Cohen ÉA. 2017. HIV-1 Vpu downmodulates ICAM-1 expression, resulting in decreased killing of infected CD4$^+$ T cells by NK cells. J Virol 91:e02442-16. https://doi.org/10.1128/JVI.02442-16.

Editor Wesley I. Sundquist, University of Utah

Copyright © 2017 American Society for Microbiology. All Rights Reserved.

Address correspondence to Éric A. Cohen, eric.cohen@ircm.qc.ca.

The *vpu* gene is found exclusively in human immunodeficiency virus type 1 (HIV-1) and several closely related simian immunodeficiency viruses (SIV) and codes for a 16- to 17-kDa nonstructural protein (1, 2). Although Vpu is not strictly required for virus

replication *in vitro*, empirical observations suggest that it is absolutely required at early stages of infection *in vivo*. All transmitter/founder (T/F) HIV-1 strains contain a functionally competent *vpu* coding sequence (3), and humanized mouse models have demonstrated the contribution of Vpu to early viral dissemination after infection (4, 5).

The HIV-1 Vpu protein is comprised of a short luminal domain, a single-pass α-helical transmembrane domain (TMD), and an approximately 56-amino-acid (aa) cytoplasmic tail comprised of two alpha-helices flanking an unstructured linker region. Two serine residues at aa 52 and 56 (S52/S56) are phosphorylated by cellular casein kinase II, resulting in recruitment of the beta-transducin repeat-containing E3 ubiquitin protein ligase (β-TrCP) component of the Skp, Cullin, F-box ($SCF^{\beta\text{-}TrCP}$) E3 ubiquitin ligase complex (6).

Vpu promotes evasion from various intrinsic, innate, and adaptive immune responses by modulating the expression of specific host plasma membrane (PM) proteins (7). By far the best-studied targets of Vpu are the HIV-1 primary receptor CD4 (8) and the host restriction factor BST2/tetherin (9, 10). Vpu targets CD4 in the endoplasmic reticulum (ER) via interactions that involve its TMD and the membrane-proximal cytoplasmic alpha-helix domain, leading to $SCF^{\beta\text{-}TrCP}$-mediated CD4 ubiquitination and degradation through the ER-associated protein degradation (ERAD) pathway (6, 8). CD4 downregulation is thought to prevent superinfection (11) and to promote release of infectious particles by limiting gp120/CD4 binding within the cell (prior to virion assembly) (12) and at the PM (13). Most importantly, premature gp120/CD4 interactions within virus-producing cells cause the unmasking of epitopes within gp120, resulting in increased vulnerability to antibody-dependent cell-mediated cytotoxicity (ADCC) (14, 15).

Vpu also counteracts BST2, an antiviral host restriction factor that strongly inhibits the release of HIV-1 and other enveloped viruses, by linking budding virions at the surface of infected cells (9, 10). Vpu targets both recycling and newly synthesized BST2 in the *trans*-Golgi network (TGN) through its TMD and removes the restriction factor from sites of virus budding via lateral displacement, intracellular sequestration, and degradation mechanisms that are dependent on the phosphorylation of the S52/S56 motif and recruitment of β-TrCP (16–18). Unlike CD4, BST2 degradation is not absolutely required for Vpu-mediated surface downregulation (19).

In recent years, a plethora of novel targets of Vpu have been discovered (reviewed in reference 7). They include immunoreceptors, such as human leukocyte antigen C (HLA-C) (20), NK-T-B antigen (NTB-A) (21), CD1d (22), and poliovirus receptor (PVR) (23); homing molecules, like CCR7 (24) and CD62L (25); sodium-coupled neutral amino acid transporter 1 (SNAT1) (26); and numerous members of the tetraspanin family (27). These downregulations lead to a wide array of immunomodulatory effects, including immune evasion and metabolic dysfunction. Interestingly, Vpu does not seem to employ redundant mechanisms to downregulate these proteins, but instead appears to act on its assorted targets at different locations within the vesicular system through various means, including intracellular sequestration and/or degradation.

Given the ever-increasing number of proteins shown to be downregulated by Vpu, we sought to identify new cell surface targets of this molecule by employing an unbiased methodology. To accomplish this, the PM proteomes from T cells either expressing Vpu or not were compared using stable isotope labeling of amino acids in cell culture (SILAC)-based mass spectrometry (MS). A similar methodology has previously been employed successfully by another group (26). In addition to corroborating several putative targets identified in the previous work, here, we identify intercellular adhesion molecule 1 (ICAM-1) and ICAM-3 as host membrane proteins downmodulated by Vpu in HIV-1-infected primary $CD4^+$ T cells. More specifically, we show that ICAM-1 mRNA expression is upregulated in HIV-1-infected cells, while Vpu counterbalances this effect by downregulating ICAM-1 protein from the cell surface. We demonstrate that Vpu interacts with ICAM-1 through its TMD and induces both ICAM-1 cell surface downregulation and proteasomal degradation via its dual-serine motif. We further show that Vpu-mediated ICAM-1 degradation relies on the recruitment of β-TrCP-1.

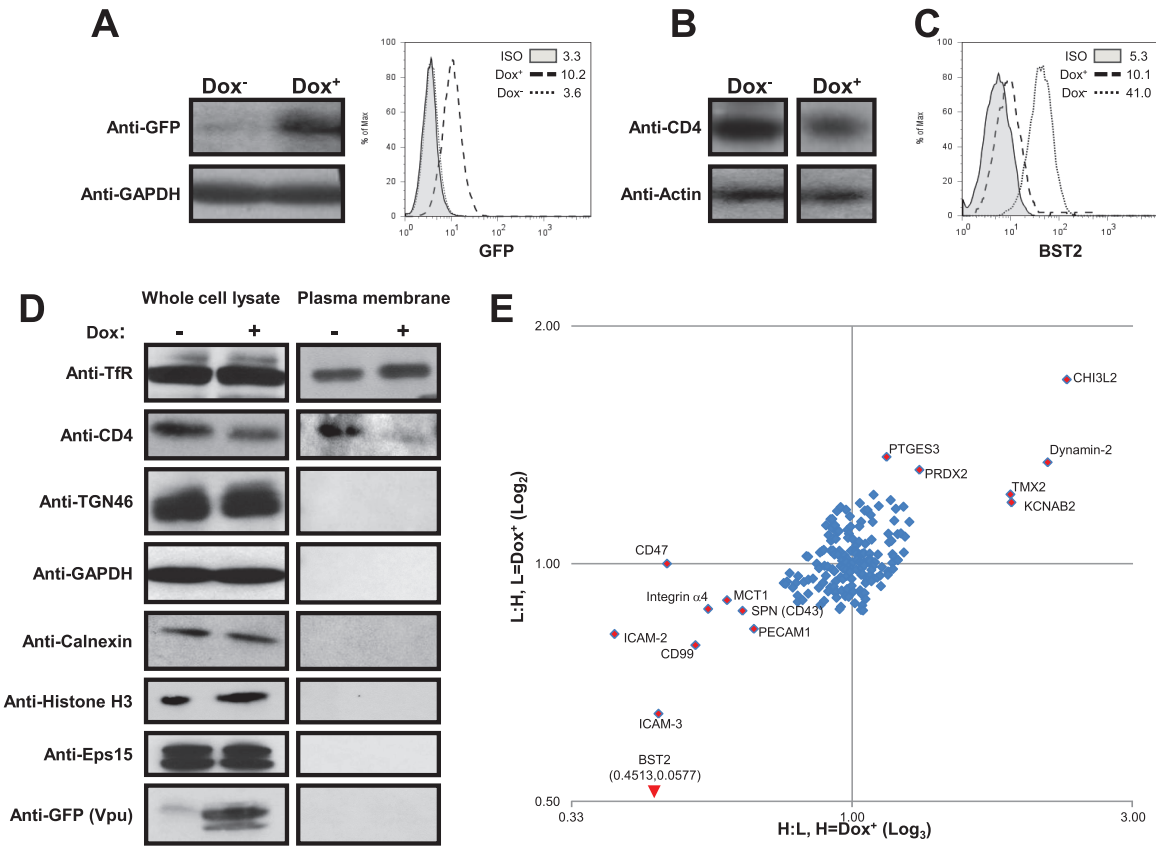

FIG 1 Identification of putative membrane-associated proteins targeted by HIV-1 Vpu. (A to C) Jurkat cells expressing a VpuGFP chimeric protein under the control of a Dox-inducible promoter (Jurkat^{TetR}VpuGFP) were characterized for VpuGFP expression and activity. Jurkat^{TetR}VpuGFP cells were left untreated (Dox^{-}) or treated with Dox (Dox^{+}) for 36 h and then analyzed for VpuGFP expression by Western blotting (A, left) and flow cytometry (A, right), for CD4 expression by Western blotting (B), and for surface BST2 expression by flow cytometry (C). (D) Plasma membranes were isolated as described in Materials and Methods. Dox^{+} and Dox^{-} Jurkat^{TetR}VpuGFP PM isolates and whole-cell lysates were separated by SDS-PAGE and analyzed for the indicated proteins by Western blotting. (E) Dox$^{+/-}$ Jurkat^{TetR}VpuGFP PM isolates were analyzed by SILAC-based MS as described in Materials and Methods. The graph shows the ratio of identified heavy-labeled proteins to light-labeled proteins (H:L) when VpuGFP was induced in heavy-labeled cells (x axis; $n = 3$) and the ratio of identified light-labeled proteins to heavy-labeled proteins (L:H) when VpuGFP was induced in light-labeled cells (y axis; $n = 3$). The coordinates of the BST2 data point exceeded the limits of the graph.

Lastly, we provide evidence that downregulation of ICAM-1 by Vpu results in the decreased formation of conjugates between infected CD4^{+} T and NK cells and reduced NK cell-mediated killing. This immune evasion mechanism may come at the cost of lowered virus infectivity.

RESULTS

SILAC mass spectrometry-based identification of novel targets of HIV-1 Vpu. Given the growing number of surface proteins known to be targeted by HIV-1 Vpu, we sought to identify novel targets of this protein. To do this, a Jurkat cell line was generated expressing HIV-1 Vpu protein fused at the C terminus to green fluorescent protein (GFP) (VpuGFP) under the control of a doxycycline (Dox)-inducible promoter (Jurkat^{TetR}VpuGFP). When treated with Dox, this cell line was shown by flow cytometry to express GFP and to produce an approximately 42-kDa fusion protein detectable by Western blotting using anti-GFP antibodies (Abs) (Fig. 1A). Furthermore, Dox treatment led to CD4 downregulation, as measured by Western blotting, and BST2 downregulation, as measured by flow cytometry (Fig. 1B and C), indicating that Dox-induced VpuGFP is biologically active.

Once validated, Jurkat^{TetR}VpuGFP cells were treated or not with Dox for 36 h, and PMs were isolated using a cationic silica-based technique (28). Briefly, cells were coated with positively charged colloidal silica beads, followed by polymerization with acrylic

acid. This treatment provides both structural integrity and mass to the PM, allowing it to be isolated by density gradient centrifugation. The quality and purity of isolated PM proteomes were verified by Western blotting of various membrane and nonmembrane proteins (Fig. 1D). To quantify membrane proteins in the presence or absence of VpuGFP, SILAC (29) was carried out on PM isolates with VpuGFP expression induced (via Dox treatment) in either light- or heavy-amino-acid-labeled cells, as described in Materials and Methods. Proteome samples were then analyzed by LTQ Orbitrap XL tandem MS (MS-MS), and MaxQuant computer software was used to quantify the relative levels of identified proteins expressed as the ratio of heavy-labeled to light-labeled proteins (H:L). Experiments were carried out three times, with Vpu expression induced in the light-labeled cell cultures and three times with Vpu expression induced in heavy-labeled cultures. As false H:L values resulting from environmental contaminants or computer errors remain consistent even when experimental labels are inverted, this methodology allowed the exclusion of these confounding factors. Identified proteins were scored according to the degree of modulation, with H:L values of 1.25 and 0.75 set as cutoff thresholds for protein dysregulation. BST2 was found to be the target most downregulated by HIV-1 Vpu, validating our methodology. In contrast, the other canonical target of Vpu, CD4, was not detected by the methodology. This is likely the result of the very low surface CD4 expression found on the Jurkat E6.1 parental cells used to generate the Jurkat^{TetR}VpuGFP cell line (30, 31). A list of putative targets was generated based on their potential impacts on immunological functions and/or contributions to HIV-1 pathogenesis (Fig. 1E; see Table S1 in the supplemental material). Several of these targets have been independently validated as downregulated by HIV-1 in a recent publication (26).

HIV-1 Vpu prevents the upregulation of ICAM-1 and ICAM-3 to the surface of primary CD4$^+$ T cells. ICAM-2 and ICAM-3 were both identified as putative candidates for Vpu-mediated surface downregulation (Fig. 1E; see Table S1 in the supplemental material). To validate our SILAC screening assay in a physiologically relevant context, we investigated the effect of HIV-1 Vpu on ICAM-3 expression in HIV-1-infected primary CD4$^+$ T cells. ICAM-1 expression was also investigated, as this molecule has already been implicated in numerous aspects of HIV infection and shares considerable functional redundancy with ICAM-2 and -3, including a common integrin binding partner, lymphocyte function-associated antigen 1 (LFA-1) (32). Furthermore, Jurkat cells express extremely low levels of ICAM-1 (33, 34), and it is likely that ICAM-1 expression is below the limit of detection by MS-MS. ICAM-2 was excluded from further analysis as, although it is expressed at relatively high levels on the Jurkat T cells used in our SILAC-based screen, it is generally considered more important for endothelial cell function (32, 33).

Primary CD4$^+$ T cells were infected with GFP-marked NL4.3 HIV-1 expressing wild-type (WT) Vpu or isogenic variants expressing either Vpu mutants lacking the conserved β-TrCP-recruiting S52/S56 motif (S52/S56D Vpu) or a triple-alanine motif within the TMD involved in BST2 interaction (35) (A10/A14/A18L Vpu), or lacking Vpu (ΔVpu). Surface expression of ICAM-1 and ICAM-3 was measured on infected cells by flow cytometry 48 h later. The expression of CD45 and BST2 was analyzed in parallel as negative and positive controls, respectively. WT HIV-1 infection resulted in a slight upregulation of ICAM-1 and ICAM-3 on the surface of infected cells. In comparison, cells infected with ΔVpu HIV-1 displayed a much larger increase in the expression of these ICAMs (Fig. 2). Therefore, although HIV-1 upregulates the surface expression of ICAMs on infected cells, this upregulation appears to be attenuated in a Vpu-dependent manner. Vpu-mediated dampening of ICAM upregulation is dependent on both the S52/S56 motif and to a lesser extent the A10, A14, and A18 residues found within the TMD, as disruption of these motifs prevents or limits this effect, respectively (Fig. 2). The effect of Vpu was more pronounced for ICAM-1 than for ICAM-3 in infected primary CD4$^+$ T cells. Given this, along with the numerous well-described roles of ICAM-1 in HIV-1 infection, we decided to focus our mechanistic investigations on ICAM-1.

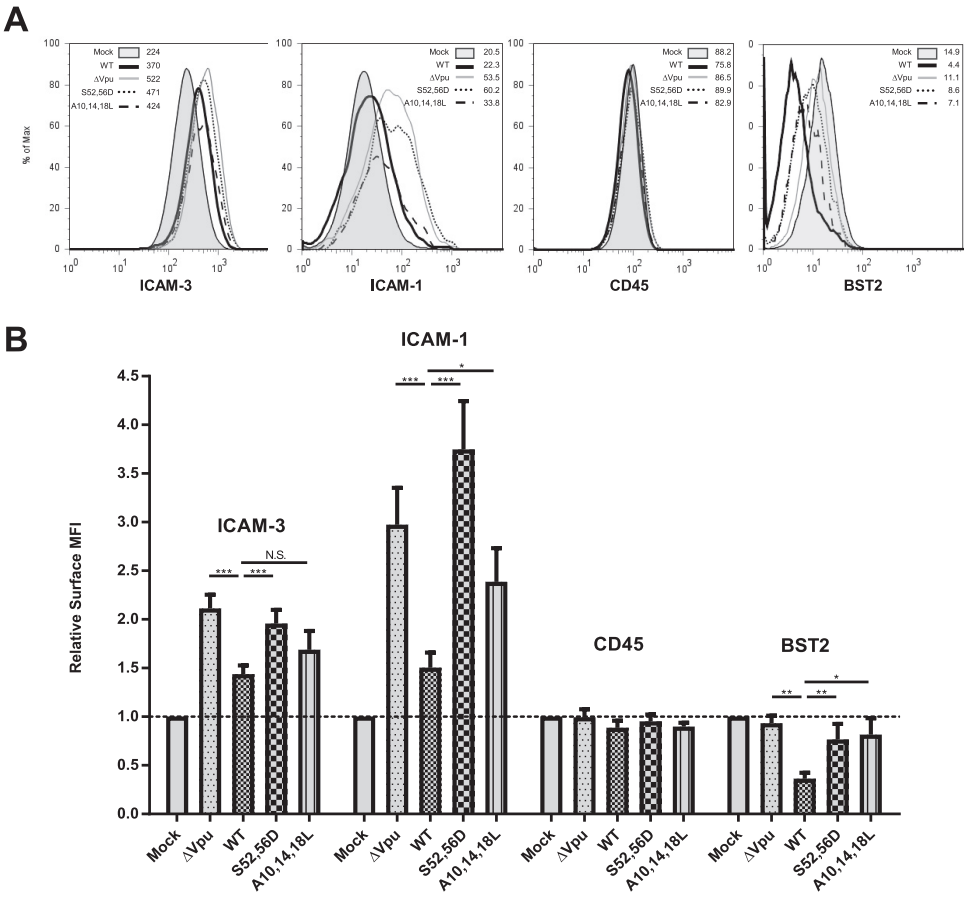

FIG 2 Vpu prevents ICAM-1 and ICAM-3 upregulation on the surface of primary CD4$^+$ T cells by a process that depends on its TMD and dual-serine motif. Primary human CD4$^+$ T cells were infected with GFP-marked NL4.3 HIV-1 either lacking Vpu (ΔVpu) or expressing wild-type Vpu (WT), Vpu lacking the dual-serine motif (S52D,56D), or Vpu lacking the TMD alanine face (A10,14,18L). Forty-eight hours postinfection, surface expression of ICAM-1, ICAM-3, CD45, and BST2 was measured on GFP$^+$ cells by flow cytometry. (A) Representative histograms. (B) Compiled data expressed as the mean fluorescence intensity (MFI) of GFP$^+$ cells normalized to the MFI of mock-infected controls ($n \geq 4$). The error bars represent standard errors of the mean (SEM). *, $P \leq 0.05$; **, $P \leq 0.01$; ***, $P \leq 0.005$; N.S., nonsignificant.

ICAM-1 is transcriptionally upregulated by HIV-1 infection, while ICAM-1 protein is reduced in the presence of Vpu. ICAM-1 is upregulated in response to numerous infections, including HIV-1 (36, 37). We therefore asked if the attenuation of ICAM-1 protein upregulation mediated by Vpu is a result of transcriptional repression. To investigate this, HeLa cells were infected for 48 h with vesicular stomatitis virus glycoprotein G (VSV-G)-pseudotyped GFP-marked WT or ΔVpu NL4.3 HIV-1. ICAM-1 protein expression was then assessed by Western blotting, and mRNA levels were measured by reverse transcription-quantitative PCR (RT-qPCR). Levels of infection were comparable for WT and ΔVpu HIV-1, as indicated by the percentages of cells expressing GFP (Fig. 3A). HIV-1 infection resulted in an approximately 7.2-fold increase in ICAM-1 transcripts compared to uninfected controls (Fig. 3B), with no difference in transcript levels observed between WT and ΔVpu HIV-1 infections. As reported previously (38), Vpu also had no effect on BST2 transcript levels.

In contrast to transcripts, whole-cell protein levels of ICAM-1 were differentially increased by infection, depending on the presence or absence of Vpu (Fig. 3C and D), with ICAM-1 expression in ΔVpu-infected cells producing 2-fold more protein than their Vpu-competent counterparts. This effect did not result from a generalized repression of membrane-associated protein levels, since transferrin receptor (TfR) protein expression was not affected by the presence of Vpu (Fig. 3C and D). The discrepancy between ICAM-1 transcript and protein regulation suggests that this molecule is upregulated

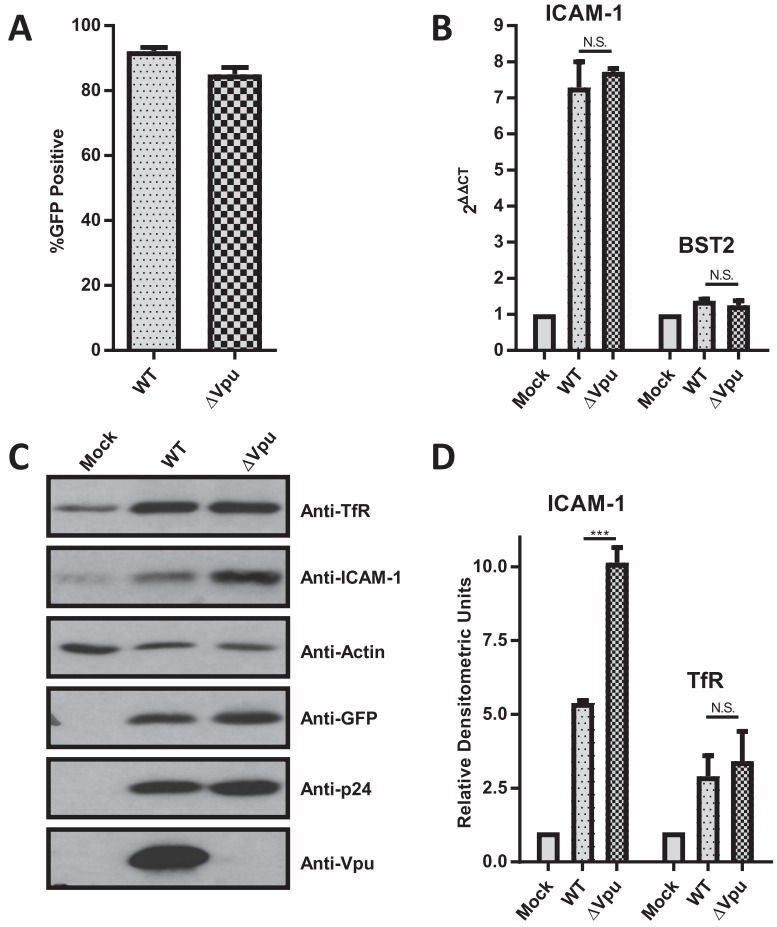

FIG 3 ICAM-1 is upregulated at the transcriptional level in response to HIV-1 infection and downregulated posttranscriptionally by Vpu. HeLa cells were infected with VSV-G-pseudotyped GFP-marked wild-type NL4.3 HIV-1 (WT) or HIV-1 lacking Vpu (ΔVpu) for 48 h ($n = 3$). (A) The percentage of cells expressing GFP was monitored by flow cytometry. (B) ICAM-1 and BST2 mRNA levels in infected cells were measured by RT-qPCR, with *gapdh* used as a reference gene. (C and D) Whole-cell lysates were analyzed for the indicated proteins by Western blotting. (C) Representative blots. (D) Compiled densitometric analysis of ICAM-1 and TfR normalized to actin and expressed relative to mock-infected controls ($n = 3$). The error bars represent SEM. ***, $P \leq 0.005$; N.S., nonsignificant.

transcriptionally as a result of HIV-1 infection while being downregulated in parallel at a posttranscriptional level through a Vpu-dependent process.

HIV-1 Vpu is sufficient to deplete ICAM-1. We next asked if Vpu alone is sufficient to decrease whole-cell ICAM-1 levels. To this end, HeLa cells were transfected with plasmids expressing either WT or mutant NL4.3 Vpu or an empty-vector control, and then surface and whole-cell ICAM-1 expression was analyzed 24 h later by flow cytometry and Western blotting, respectively. Both surface and whole-cell ICAM-1 expression was downregulated by WT Vpu but unaffected by a dual-serine-motif Vpu mutant (VpuS52/S56N) or by a mutant of Vpu that harbors a randomized TMD (VpuRD) (Fig. 4A to D). In contrast, TfR protein levels were unaltered by Vpu expression. Vpu is therefore sufficient to downregulate surface and whole-cell endogenous ICAM-1.

To confirm that Vpu-mediated ICAM-1 downregulation is a feature conserved among primary Vpu variants, experiments were repeated using various primary Vpu isolates (Fig. 4E shows Vpu sequence alignments). First, we infected primary $CD4^+$ T cells and measured ICAM-1 surface expression, as shown in Fig. 2, using a chimeric NL4.3 virus expressing Vpu from the primary ADA isolate (ADA-NL4.3). Infection with ΔVpu ADA-NL4.3 resulted in a >4-fold increase in surface ICAM-1 expression relative to the mock-infected control, while Vpu-competent ADA-NL4.3 infection increased ICAM-1 surface expression by only approximately 2-fold (Fig. 4F).

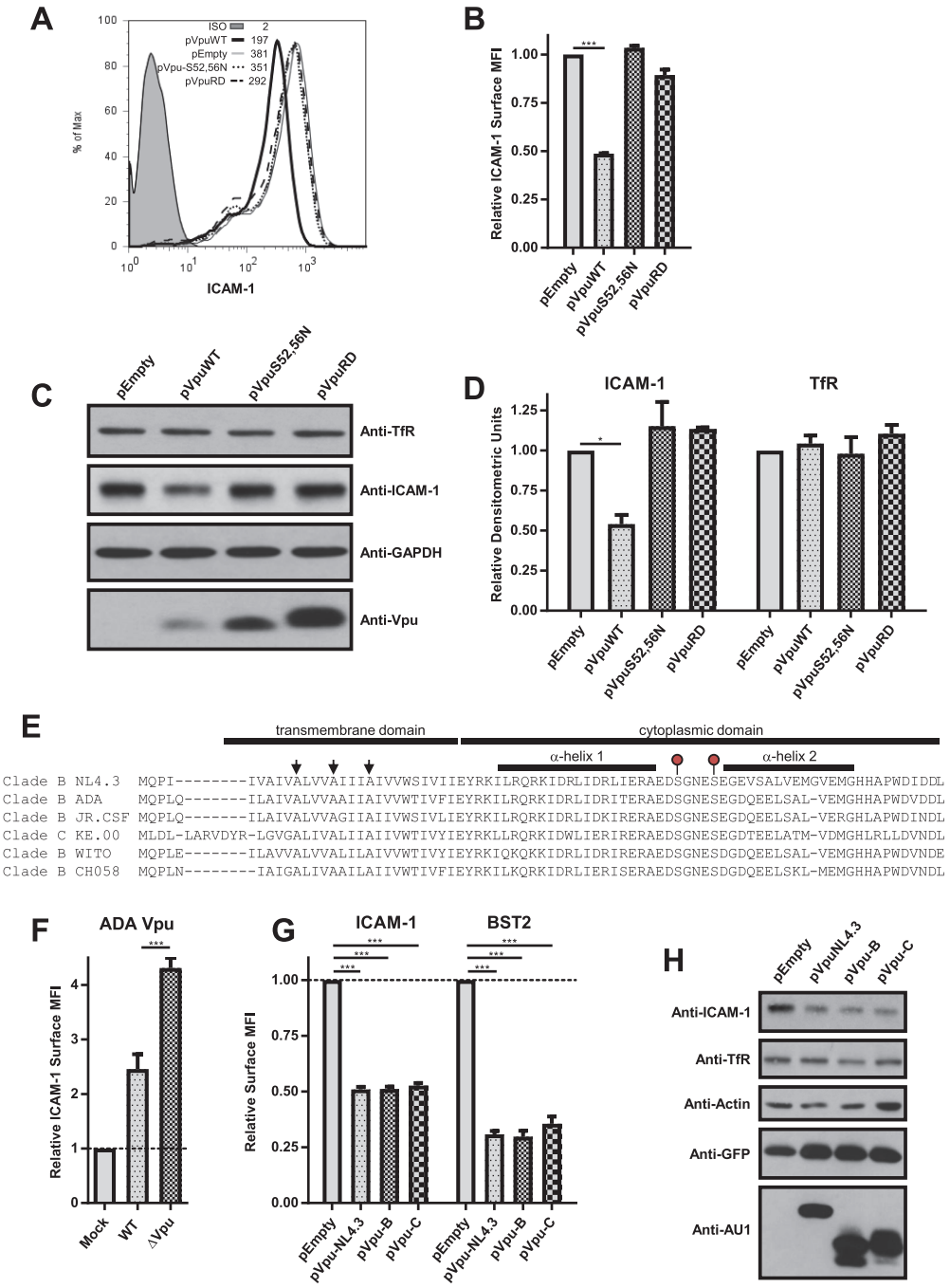

FIG 4 Vpu is sufficient to deplete endogenous ICAM-1 in a TMD- and dual-serine-motif-dependent manner. HeLa cells were transfected to express wild-type NL4.3 Vpu (pVpuWT), a mutant Vpu lacking the dual-serine motif (pVpuS52,56N), a mutant Vpu containing a randomized TMD (pVpuRD), or an empty-vector control (pEmpty) for 24 h. (A and B) Surface expression of ICAM-1 was measured by flow cytometry. (A) Representative histograms of surface ICAM-1 expression. (B) Compiled data expressed as the MFI of GFP$^+$ cells normalized to pEmpty transfections ($n \geq 3$). (C and D) Whole-cell lysates were analyzed for the indicated proteins by Western blotting. (C) Representative blots. (D) Compiled densitometric analysis of ICAM-1 and TfR blots normalized to GAPDH and expressed relative to pEmpty controls ($n = 2$). (E) Sequence alignment of all Vpu variants tested for ICAM-1 downregulation. Structural domains are indicated above, with NL4.3 used as a consensus sequence. The arrows indicate alanine residues involved in BST2 binding. The circles indicate serine phosphorylation sites required for β-TrCP binding. (F) Primary human CD4$^+$ T cells were infected with GFP-marked WT HIV-1 or HIV-1 lacking Vpu (ΔVpu) from the ADA-NL4.3 chimeric virus expressing ADA Vpu from an NL4.3 backbone (ADA Vpu). Surface expression of ICAM-1 was measured by flow cytometry ($n = 5$). The data are expressed as the MFI of GFP$^+$ cells relative to the MFI of mock-infected controls. (G and H) HeLa cells were transfected with GFP-marked plasmids expressing WT NL4.3 Vpu (pVpuNL4.3), Vpu variants from clade B or C HIV-1 primary isolates (pVpu-B [JR-CSF] or pVpu-C [KE.00], respectively), or an empty-vector control expressing GFP alone (pEmpty) for 24 h. (G) Surface expression of ICAM-1 and BST2 was measured by flow cytometry ($n = 3$). The data are expressed as the MFI of GFP$^+$ cells relative to the MFI of GFP$^+$ cells from pEmpty

(Continued on next page)

In contrast to many primary isolates and T/F Vpu variants, NL4.3 Vpu has recently been shown to be unable to downregulate HLA-C from the surface of infected primary $CD4^+$ T cells (20), and it has been stressed that NL4.3 Vpu may not accurately reflect many primary HIV-1 Vpu variants with regard to certain functions. To investigate whether primary Vpu variants are also sufficient to downregulate ICAM-1 protein, HeLa transfection experiments were repeated using plasmids coexpressing GFP with AU1-tagged primary Vpu variants from either clade B (JR-CSF) or clade C (KE.00) group M HIV-1 (39). Similar to transfection with laboratory-adapted NL4.3 Vpu, transfection with Vpu from primary B clade or C clade isolates resulted in decreased ICAM-1 surface and whole-cell protein expression (Fig. 4G to H). Similar decreases in ICAM-1 expression were also observed in HeLa cells upon transfection with primary T/F Vpu variants capable of downregulating surface HLA-C expression (reference 20 and data not shown). Taken together, our results demonstrate that Vpu-mediated ICAM-1 downregulation is an activity conserved among primary Vpu variants.

Vpu interacts with ICAM-1 and targets it for proteasomal degradation. We questioned whether Vpu might physically associate with ICAM-1 to induce its depletion. HeLa cells were infected with VSV-G-pseudotyped GFP-marked WT; ΔVpu; or A10/A14/A18L Vpu NL4.3 HIV-1 for 48 h before ICAM-1 was immunoprecipitated and the immunoprecipitates were analyzed for the presence of Vpu by Western blotting. In this system, WT Vpu was detected in immunoprecipitates of ICAM-1, whereas the TMD mutant A10/A14/A18L Vpu was not, despite greater ICAM-1 pulldown in A10/A14/A18L Vpu NL4.3-infected samples (Fig. 5A). In agreement with this, input control lanes demonstrated that A10/A14/A18L Vpu does not deplete ICAM-1 in infected HeLa cells. These results indicate that ICAM-1 is able to associate specifically with HIV-1 Vpu and suggest that this interaction occurs via the TMD of Vpu.

We next sought to determine whether Vpu accelerates ICAM-1 protein turnover by either the proteasomal or lysosomal route. To this end, the stability of ICAM-1 protein in the presence or absence of Vpu was investigated by pulse-chase analysis. HeLa cells were transfected with either Vpu-expressing or control plasmids for 22 h; starved for 45 min in cysteine- and methionine-free medium in the presence or absence of either the proteasome inhibitor MG132 or concanamycin A (CMA), an H^+ ATPase inhibitor that prevents lysosomal acidification; and then pulse-labeled with ^{35}S-labeled amino acids for 1 h before initiating a chase, as indicated (Fig. 5B and C). Two forms of ICAM-1 are detectable by pulse-chase analysis: a lower-molecular-mass form (~65 kDa) representing an immature hypoglycosylated ICAM-1 variant, and a higher-molecular-mass form (~90 kDa) representing the mature protein found at the cell surface (40).

In the absence of inhibitors, HeLa cells transfected with control plasmids showed increased expression of the mature form of ICAM-1 over the first hour of chase with no significant change in the expression of the immature form (Fig. 5B and C, top). Over the following 3 h, immature ICAM-1 levels decreased to about 50% of their original value, while the quantity of mature ICAM-1 remained higher than that seen at the initiation of the chase (time zero). Taken together, these data suggest that endogenous ICAM-1 continues to transition from its ER-localized immature form to its surface-bound mature form over the 4 h of the chase experiment. In contrast, the presence of Vpu resulted in no appreciable increase in the mature form of ICAM-1 over the 4-h chase period and induced an accelerated loss of immature ICAM-1 protein compared to controls (Fig. 5B and C, top). Vpu therefore appears to accelerate the loss of ICAM-1 at the protein level, preferentially acting upon the immature form of ICAM-1 and causing a decrease in mature ICAM-1 levels by proxy. Treatment of cells with MG132 prevented the Vpu-mediated accelerated loss of both mature and immature ICAM-1 (Fig. 5B and C, middle). In contrast, treatment of cells with CMA did not significantly alter the effects of Vpu on

FIG 4 Legend (Continued)
transfections. (H) Whole-cell lysates were separated by SDS-PAGE and analyzed for the indicated proteins by Western blotting. A representative of 3 experiments is shown. The error bars represent SEM. *, $P \leq 0.05$; ***, $P \leq 0.005$.

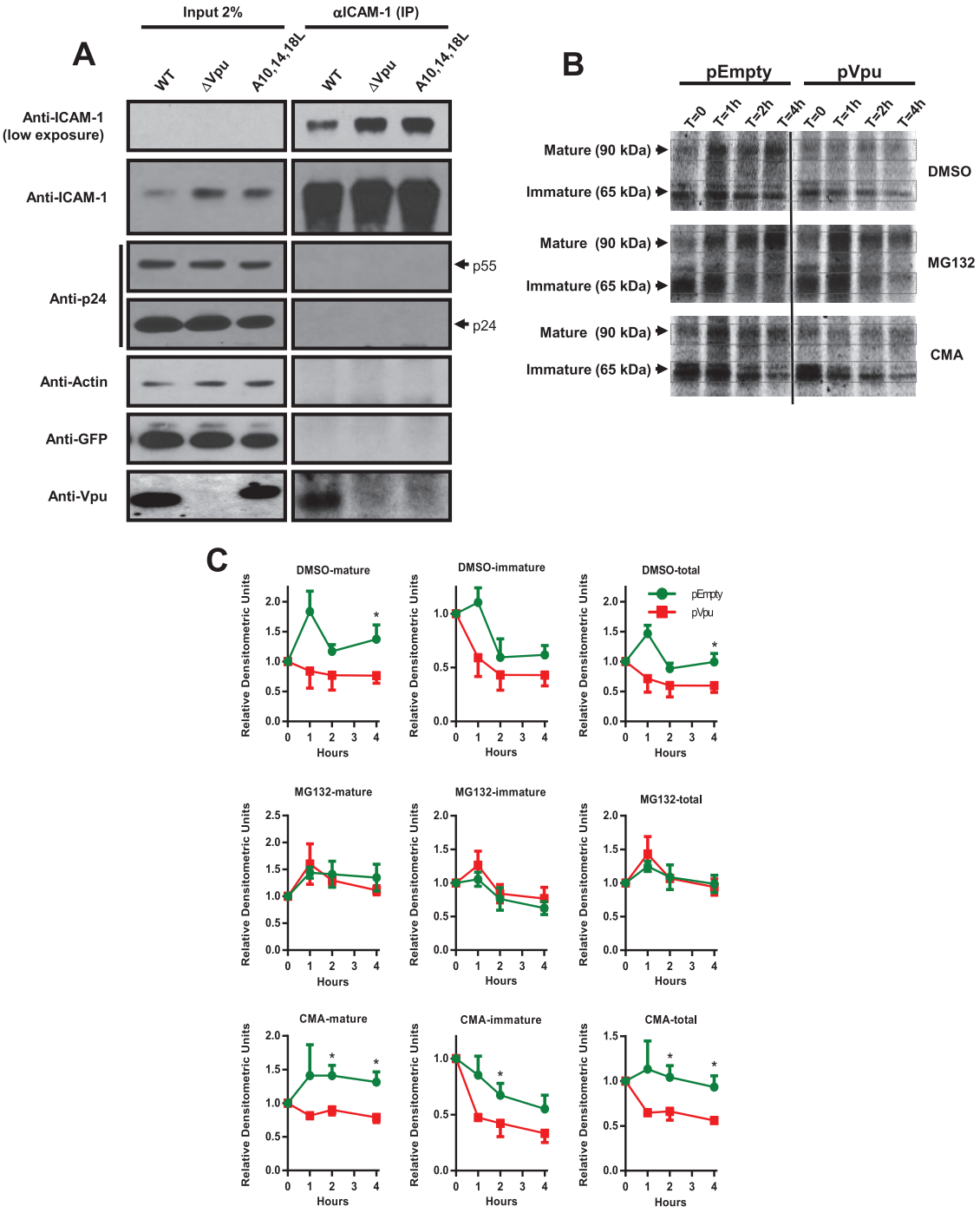

FIG 5 Vpu interacts with ICAM-1 and induces its turnover in a proteasome-dependent manner. (A) HeLa cells were infected with VSV-G-pseudotyped GFP-marked wild-type (WT); Vpu-deficient (ΔVpu); or A10/A14/A18L Vpu (A10,14,18L) NL4.3 HIV-1 for 48 h prior to cell lysis and immunoprecipitation (IP) using anti-ICAM-1 Abs. The immunoprecipitates were analyzed for the indicated proteins by Western blotting. (B and C) HeLa cells were transfected to express wild-type NL4.3 Vpu (pVpu) or an empty-vector control (pEmpty) for 22 h. The cells were then pulse-labeled with ^{35}S-labeled amino acids for 1 h and chased for the indicated times in the presence or absence of MG132 or CMA. Whole-cell lysates were immunoprecipitated with anti-ICAM-1 Abs. (B) Representative phosphorimages. The bands of interest are indicated. DMSO, dimethyl sulfoxide. (C) Relative quantification using quantitative scanning of ICAM-1 bands. The relative amount of ICAM-1 remaining over time compared to time zero is plotted for each condition ($n \geq 3$). The error bars represent SEM. *, $P \leq 0.05$.

ICAM-1 protein stability (Fig. 5B and C, bottom). Overall, these results indicate that Vpu accelerates ICAM-1 protein turnover in a proteasome-dependent manner. Furthermore, the observation that Vpu accelerates the loss of immature ICAM-1 protein suggests that Vpu targets ICAM-1 at the ER.

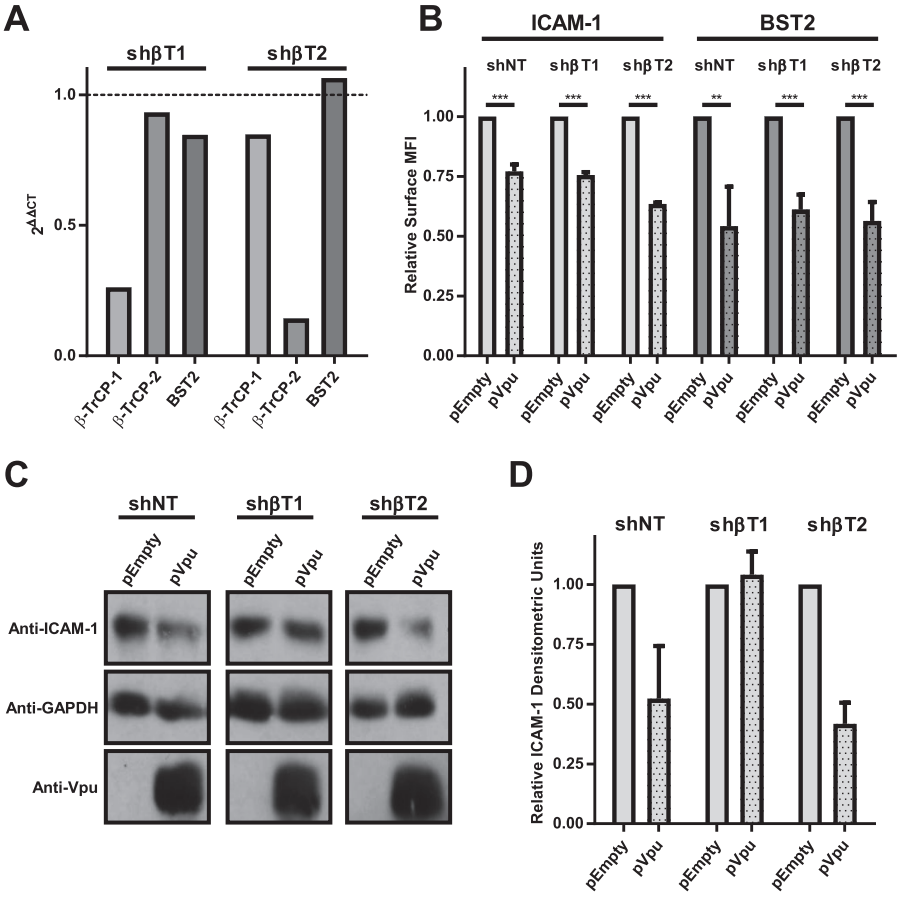

FIG 6 Vpu dual-serine-motif-dependent surface ICAM-1 downregulation is dissociable from β-TrCP-1-mediated ICAM-1 degradation. (A) Expression of β-TrCP-1, β-TrCP-2, and BST2 mRNA transcripts was evaluated by RT-qPCR in HeLa cells expressing nontargeting shRNA (shNT) or shRNA against either β-TrCP-1 (shβT1) or β-TrCP-2 (shβT2). Data were expressed relative to the value for the shNT control. *gapdh* was used as a reference gene. (B to D) shNT, shβT1, and shβT2 HeLa cells shNT, shT1, and TrCP-2 were transfected with plasmids expressing wild-type NL4.3 Vpu (pVpu) or an empty-vector control (pEmpty) for 24 h. (B) Surface expression of ICAM-1 and BST2 was measured by flow cytometry ($n = 3$). The data are expressed as the MFI of Vpu-transfected cells normalized to the MFI of cells from pEmpty transfections. (C and D) Whole-cell lysates were analyzed for the indicated proteins by Western blotting. (C) Representative blots. (D) Compiled densitometric analysis of ICAM-1 normalized to GAPDH ($n = 2$). **, $P \leq 0.01$; ***, $P \leq 0.005$.

β-TrCP-1 is required for Vpu-mediated ICAM-1 degradation, but not ICAM-1 surface downregulation. Given the requirement for the β-TrCP-recruiting S52/S56 motif of Vpu for ICAM-1 downregulation, as well as the accelerated loss of ICAM-1 induced by Vpu, we questioned whether β-TrCP is essential for both ICAM-1 surface downregulation and degradation. Two forms of β-TrCP are found in humans (41). To investigate their individual requirements, we transfected HeLa cells stably expressing short hairpin RNA (shRNA) against β-TrCP-1, β-TrCP-2, or a nontargeting shRNA control with Vpu expressor plasmids. Cells were analyzed by flow cytometry 24 h later for surface ICAM-1 expression, while whole-cell ICAM-1 levels were analyzed by Western blotting. Knockdown of β-TrCP-1/2 expression was confirmed by RT-qPCR analysis (Fig. 6A).

Surprisingly, although the β-TrCP-binding S52/S56 motif is required for ICAM-1 downregulation (Fig. 2 and 4), ICAM-1 surface downregulation was maintained in HeLa cells expressing shRNA against either β-TrCP-1 or -2 (Fig. 6B, left). As previously reported (42), Vpu-mediated BST2 surface downregulation was also unaffected by β-TrCP-1/2 depletion (Fig. 6B, right). With regard to whole-cell protein levels, however, the quantity of ICAM-1 protein was not reduced by Vpu in HeLa cells expressing shRNA targeting β-TrCP-1, yet depletion was maintained in HeLa cells expressing nontargeting

shRNA or shRNA targeting β-TrCP-2 (Fig. 6C and D). Hence, as reported for Vpu-mediated BST2 antagonism (43), our results indicate that the S52/S56 motif of Vpu plays two unique and dissociable roles, being required for ICAM-1 surface downregulation in the absence of β-TrCP-1-mediated protein depletion.

Vpu decreases particle infectivity by decreasing the level of ICAM-1 packaged into virions. ICAM-1 has previously been shown to be selectively packaged into HIV-1 virions to increase their infectivity, with the amount of packaged ICAM-1 correlating with its cell surface expression (44). We therefore assessed whether Vpu-mediated ICAM-1 cell surface downregulation might decrease virus infectivity by lowering the amount of ICAM-1 packaged into virions.

First, we confirmed that Vpu is sufficient to affect exogenous ICAM-1 expression in HEK 293T cells. ICAM-1 or TfR expressor plasmids were used to transfect HEK 293T cells, and GFP-marked Vpu expressor plasmids were cotransfected at increasing concentrations. Expression of Vpu in HEK 293T cells resulted in a dose-dependent decrease in ICAM-1 protein (Fig. 7A). Vpu also induced the accumulation of the lower-molecular-mass form of ICAM-1 (~65 kDa), which was also sensitive to Vpu-mediated depletion at higher Vpu input. Comparable results were seen for ICAM-3 (data not shown). In contrast, no reduction of TfR expression was observed upon increased Vpu expression compared to GFP-only vector controls. Furthermore, no immature form of TfR could be detected by Western blotting, suggesting that Vpu overexpression was not causing a general obstruction of the secretory system. In total, these results suggest that Vpu acts specifically to downregulate ICAM-1 expression in HEK 293T cells, as well as to inhibit the transition of ICAM-1 from the immature form found in the ER to the fully glycosylated form found at the cell surface.

To investigate the effects of Vpu on ICAM-1 incorporation into nascent HIV-1 virions, HEK 293T cells were transfected with WT, ΔVpu, or S52/S56D Vpu NL4.3 proviruses in conjunction with ICAM-1 expressor plasmids. ICAM-1 incorporation into released HIV-1 particles was examined by Western blotting 48 h later. The presence of WT Vpu, but not S52/S56D Vpu, resulted in decreased expression of mature ICAM-1 in cell lysates, which corresponded to decreased incorporation of mature ICAM-1 into HIV-1 virions (Fig. 7B and C). Vpu therefore appears to lower the incorporation of ICAM-1 into HIV-1 particles by downregulating the adhesion molecule from the surface of virus-producing cells. Importantly, no change in the amount of virus-associated p24 was detected in the presence or absence of Vpu, indicating that ICAM-1 has no effect on virion release. Moreover, although some experiments showed a trend toward increased gp120 levels in ΔVpu virions (Fig. 7B), quantitative analysis over several experiments revealed no significant change in gp120 levels in released WT and Vpu mutant virions (Fig. 7C), in line with previous reports demonstrating that ICAM-1 levels do not affect Env packaging or processing (45, 46).

To examine the effect of Vpu-mediated decreased ICAM-1 incorporation on viral infectivity, ICAM-1-expressing WT, ΔVpu, or S52/S56D Vpu HIV-1 particles were normalized by p24 enzyme-linked immunosorbent assay (ELISA) and used to infect Jurkat-1G5 and Tzm-bl cell lines, which both contain stably integrated HIV long terminal repeat (LTR)-luciferase constructs (47, 48), and infectivity was evaluated by luciferase assay. Consistent with reports indicating that ICAM-1 packaging increases viral infectivity (44), ΔVpu and S52/S56D Vpu HIV-1 particles produced from ICAM-1$^+$ HEK 293T cells were more infectious (approximately 2-fold) than their Vpu-competent counterparts when Jurkat-1G5 cells were used as targets. This Vpu-mediated modulation of viral infectivity was not observed when virions were produced in the absence of ICAM-1 or when Tzm-bl cells, which do not express the ICAM-1 counterreceptor, LFA-1 (46), were used as targets (Fig. 7D).

To observe the effect of Vpu on virion infectivity in a more physiologically relevant context, WT or ΔVpu viruses were harvested from the ICAM-1$^+$ SupT1 and CEM-shBST2 T cell supernatants and evaluated for infectivity as described above using the LFA-1$^+$ Jurkat-1G5 and CEM-luc reporter cells, respectively, as targets. SupT1 and CEM-shBST2 cells were chosen for virus production, as they do not express BST2 and therefore

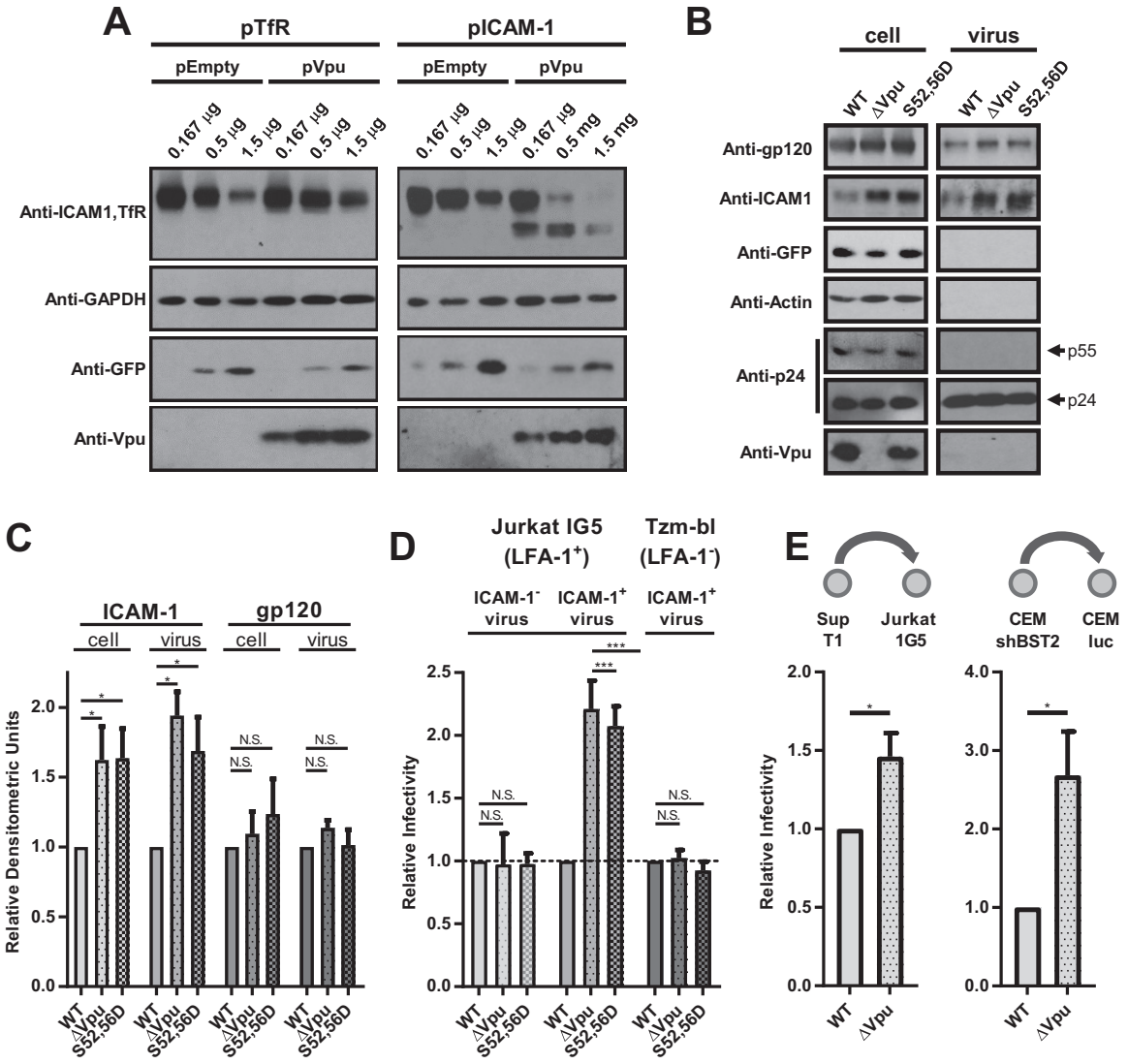

FIG 7 Vpu lowers viral infectivity by decreasing the amount of mature ICAM-1 packaged into HIV-1 virions. (A) HEK 293T cells were cotransfected with plasmids encoding ICAM-1 (pICAM-1) or TfR (pTfR), along with GFP-marked plasmids expressing wild-type NL4.3 Vpu (pVpu) or an empty-vector control expressing GFP alone (pEmpty). Twenty-four hours posttransfection, whole-cell lysates were analyzed for the indicated proteins by Western blotting. (B and C) HEK 293T cells were cotransfected with pICAM-1, along with either WT, Vpu-deficient (ΔVpu), or S52/S56D Vpu (S52, S56D) NL4.3 provirus for 48 h. Cells and virions were then pelleted and lysed prior to analysis for the indicated proteins by Western blotting. (B) Representative blots. (C) Compiled densitometric analysis of ICAM-1 and gp120 blots. Cell lysates were normalized to the amount of Gag per cell [(p24 + p55)/actin] to control for transfection efficiency. The virus lysates were normalized to p24. The results are expressed relative to the WT-infected condition ($n \geq 3$). (D) Jurkat-1G5 or HeLa Tzm-bl cells expressing luciferase under the control of the HIV-1 LTR promoter were infected for 48 h with WT, ΔVpu, or S52/S56D Vpu (S52,56D) NL4.3 viruses produced from HEK 293 T cells expressing ICAM-1 or not. Luciferase activity was calculated by measuring relative light units (RLU) from cell lysates. Relative infectivity is expressed as RLU normalized to WT-infected cells ($n \geq 3$). (E) Jurkat-1G5 or CEM-luc cells expressing luciferase under the control of the HIV-1 LTR promoter were infected for 48 h with WT or ΔVpu NL4.3 viruses produced from SupT1 or CEM-shBST2 cells, respectively. Luciferase activity was calculated by measuring RLU from cell lysates. Relative infectivity is expressed as RLU normalized to WT-infected cells ($n = 3$). A schematic representation of producer/reporter cell pairs is shown above the corresponding graphs. The error bars represent SEM. *, $P \leq 0.05$; ***, $P \leq 0.005$; N.S., nonsignificant.

remove the potential confounding effects of this restriction factor. As observed with HEK 293T-produced virions, removal of Vpu resulted in increased particle infectivity, ranging from approximately 1.5- to 2.5-fold depending on the system used (Fig. 7E).

Notably, ICAM-3 has previously been shown not to affect virion infectivity (49), and indeed, we observed minimal packaging of ICAM-3 into HIV-1 virions, as well as no effect of ICAM-3 on HIV-1 particle infectivity (data not shown).

Vpu-mediated ICAM-1 downregulation prevents NK cells from targeting HIV-1-infected primary CD4$^+$ T cells. The observed decrease in HIV-1 infectivity provided

by Vpu appears counterintuitive, as this effect is likely to limit HIV-1 transmission and/or spread during natural infection. We therefore reasoned that the apparent loss of viral fitness resulting from decreased particle infectivity may be counterbalanced by a second, fitness-increasing effect. ICAM-1 is a prerequisite for the strong cell-to-cell adhesion needed to form immunological-synapse (IS) structures (50). We therefore postulated that Vpu-mediated decreased ICAM-1 expression may result in decreased cell-to-cell conjugation with immune cells through disruption of IS structures.

To investigate the effect of Vpu on the binding of immune cells to HIV-1-infected $CD4^+$ T cells, we employed a flow cytometry-based conjugation assay (51). Briefly, a matching number of WT or ΔVpu GFP^+ NL4.3 HIV-1-infected primary $CD4^+$ T cells were sorted by fluorescence-activated cell sorting (FACS) to nearly 100% purity and then cocultured with eFluor 670-labeled autologous NK cells for 10 min before the cells were abruptly fixed with 2% paraformaldehyde (PFA). NK cell-T cell conjugates were defined as GFP^+ eFluor 670^+ events via flow cytometry. By this method, conjugation events could readily be detected when $CD4^+$ T cells were infected with HIV-1, with the number of conjugates correlating positively with the effector-to-target (E:T) ratio (Fig. 8A and B). Importantly, the absence of Vpu resulted in an approximate doubling in the number of infected $CD4^+$ T cells detected in conjugation with NK cells. Hence, Vpu decreases the formation of conjugates between NK cells and HIV-1-infected $CD4^+$ T cells.

To examine the role of ICAM-1 in the binding of NK cells to HIV-1-infected $CD4^+$ T cells, the flow cytometry-based conjugation assay was repeated in the presence of anti-ICAM-1 or anti-ICAM-3 blocking Abs (52). In this experiment, the human NK-like YTS cell line was used to compensate for the interdonor variability of primary NK cells. S52/S56D Vpu was included as a negative control, since this mutant does not downregulate ICAM-1 (Fig. 8C and D). Similar to what was observed in the absence of Abs, treatment of $CD4^+$ T cells with isotype control Abs resulted in greater NK cell-$CD4^+$ T cell conjugate formation in the context of HIV infections lacking WT Vpu protein (compare Fig. 8B to D). Treatment of infected $CD4^+$ T cells with ICAM-1 blocking Abs resulted in a general reduction in NK cell-$CD4^+$ T cell conjugate formation, as well as a loss of significant discrepancy between the number of conjugates formed in WT, ΔVpu, or S52/S56D Vpu coculture systems (Fig. 8C and D). In contrast, treatment of WT HIV-1-infected $CD4^+$ T cells with ICAM-3 blocking Abs had no effect on conjugate formation yet decreased conjugation slightly in the context of infected cells lacking a fully functional Vpu protein. ICAM-3 may therefore contribute to conjugate formation to a lesser extent than ICAM-1, and only when surface ICAM-3 levels are relatively high (i.e., in the absence of Vpu).

To determine whether lowered ICAM-1-mediated conjugation in the presence of Vpu results in decreased NK cell-mediated killing, we investigated the effects of Vpu on NK cell-induced specific lysis of HIV-1-infected $CD4^+$ T cells in the presence or absence of anti-ICAM-1 blocking Abs. To do this, matching numbers of $CD4^+$ T cells were infected with WT, ΔVpu, or S52/S56D Vpu NL4.3 HIV-1 to comparable levels of infection (~10%) and then cocultured with autologous NK cells in the presence of either anti-ICAM-1 blocking Abs or isotype control Abs for 5 h. The percent specific lysis of infected $CD4^+$ T cells was calculated from the difference in the percentage of GFP^+ $CD4^+$ T cells after NK cell coculture and the percentage of GFP^+ $CD4^+$ T cells in parallel cultures to which NK cells were not added (Fig. 9A to C) (see Materials and Methods for more details). Consistent with NK cell-$CD4^+$ T cell conjugation data, in the presence of isotype control Abs, WT Vpu decreased the NK cell-induced loss of infected $CD4^+$ T cells by approximately 1.5-fold relative to the ΔVpu and S52/S56D Vpu mutants (Fig. 9D), and treatment with anti-ICAM-1 blocking Abs decreased the total degree of $CD4^+$ T cell loss under all conditions, as well as eliminating any significant discrepancy between the levels of $CD4^+$ T cell killing in the presence or absence of functional Vpu. Taken together, these results indicate that Vpu protects HIV-1-infected $CD4^+$ T cells against NK cell conjugation and deletion in an ICAM-1-dependent manner.

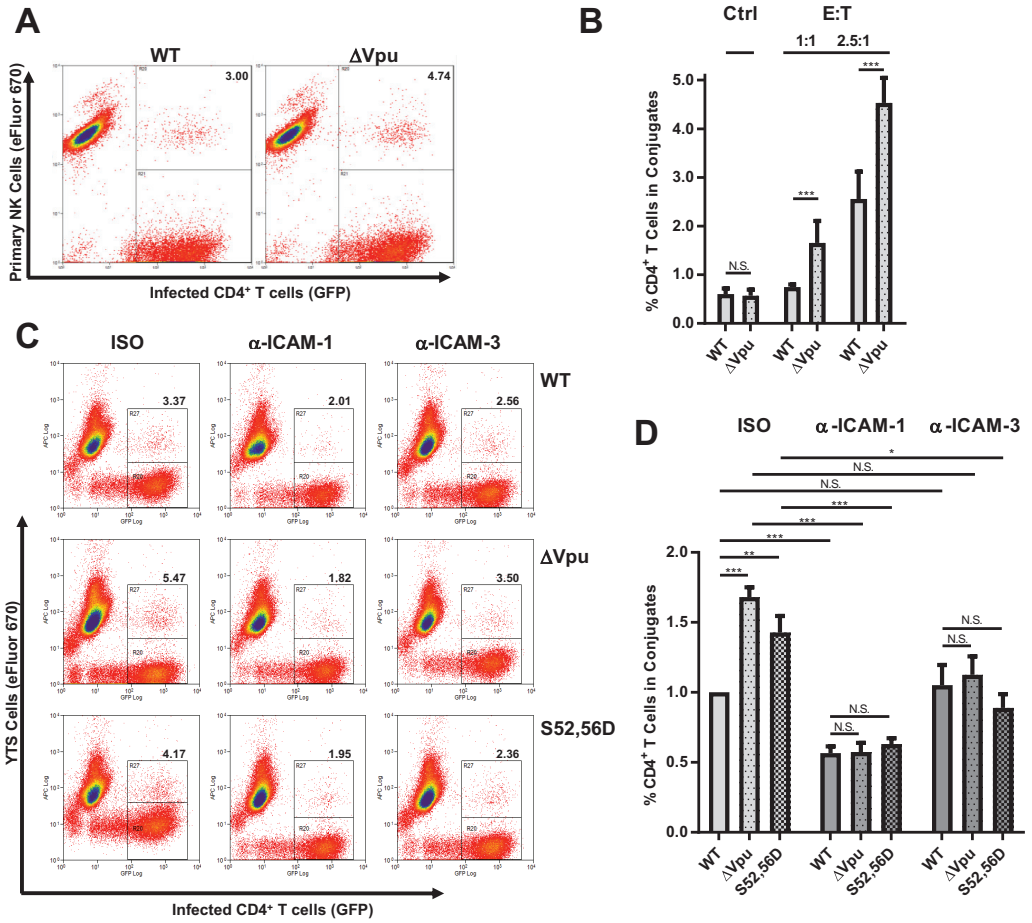

FIG 8 Vpu-induced ICAM-1 downregulation prevents NK cell conjugation to HIV-1-infected CD4$^+$ T cells. (A and B) Sorted GFP$^+$ WT or Vpu-deficient (ΔVpu) HIV-1-infected primary CD4$^+$ T cells were cocultured with eFluor 670-labeled autologous NK cells at different E:T ratios, and conjugate formation was measured by flow cytometry. (A) Representative dot plots at an E:T ratio of 2.5:1. The percentages of GFP$^+$ event that were also eFluor 670$^+$ are shown in the upper right corners. (B) Compiled data expressed as the percentage of GFP$^+$ eFluor 670$^+$ events out of total GFP$^+$ events ($n \geq 4$). As a control (Ctrl), 2% PFA was added to NK cells to fix them prior to CD4$^+$ T cell coculture. Any remaining conjugation events were assumed to be the result of a nonspecific process. (C and D) Sorted GFP$^+$ WT, Vpu-deficient (ΔVpu), or S52/S56D Vpu (S52,56D) NL4.3 HIV-1-infected primary CD4$^+$ T cells were cocultured with eFluor 670-labeled YTS cells at an E:T ratio of 3:1 in the presence of either ICAM-1 blocking Abs (α-ICAM-1), ICAM-3 blocking Abs (α-ICAM-3), or isotype control Abs (ISO). (C) Representative dot plots. The percentages of GFP$^+$ events that were also eFluor 670$^+$ are shown in the upper right corners. (D) Compiled data expressed as the percentage of GFP$^+$ eFluor 670$^+$ events out of total GFP$^+$ events relative to the WT isotype Ab-treated samples ($n \geq 3$). The error bars represent SEM. *, $P \leq 0.05$; **, $P \leq 0.01$; ***, $P \leq 0.005$; N.S., nonsignificant.

DISCUSSION

HIV-1 Vpu is a nonstructural protein that appears to be functionally dedicated to the modulation of host membrane-associated protein levels at the PM. Canonically known for CD4 and BST2 downregulation, the list of cell surface proteins targeted by Vpu has grown significantly in recent years (7, 26, 53). With this in mind, we sought to characterize the effects of this HIV-1 accessory protein on the composition of the cell surface proteome in an unbiased and comprehensive manner. Using SILAC-based MS on PM protein isolates, we identified a suite of novel putative targets of HIV-1 Vpu.

Recently, a similar study, which differed from our own in several respects, has been published by Matheson et al. (26). Matheson et al. employed a biotin-streptavidin-based technique to isolate PM glycoproteins via pulldown, whereas our study employed a method based on cationic colloidal silica beads to increase the mass and strength of PMs prior to enrichment of whole PMs by centrifugation. In addition, Matheson et al. employed the CEM T4 CD4$^+$ T cell line infected with WT virus to uncover host proteins downregulated by general infection and then repeated their

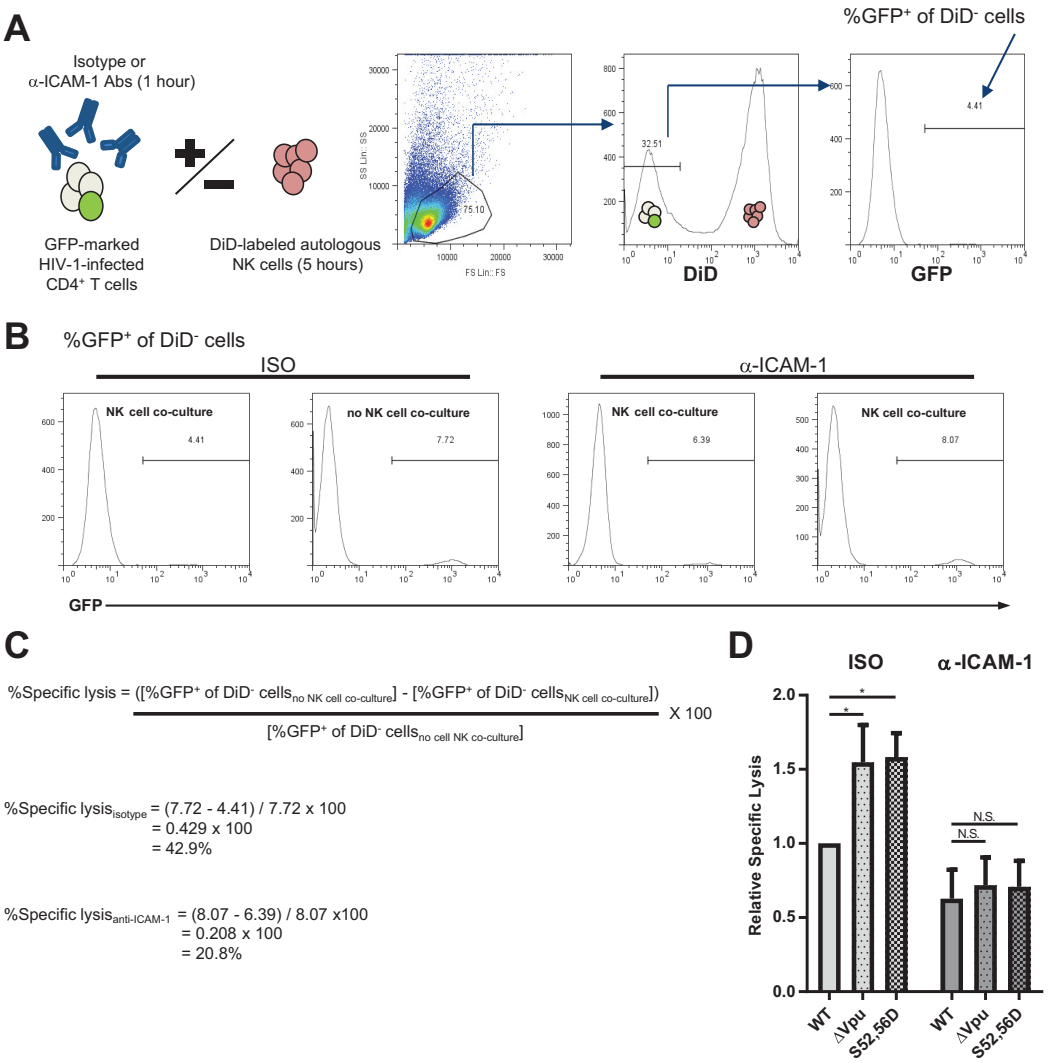

FIG 9 Vpu-induced ICAM-1 downregulation prevents NK cell-mediated killing of HIV-1-infected CD4$^+$ T cells. Primary CD4$^+$ T cells infected with GFP-marked WT, Vpu-deficient (ΔVpu), or S52/S56D Vpu (S52,56D) NL4.3 HIV-1 were cocultured with DiD-labeled autologous NK cells in the presence of ICAM-1 blocking Abs (α-ICAM-1) or isotype control Abs (ISO), and the percent specific lysis of HIV-1-infected CD4$^+$ T cells was calculated by flow cytometry. (A) Experimental design and gating strategy. HIV-1-infected CD4$^+$ T cells were pretreated for 1 h with either isotype or anti-ICAM-1 Abs before being left untreated or being cocultured with autologous, DiD dye-marked NK cells at an E:T ratio of 3:1 for 5 h. The percent GFP expression on CD4$^+$ T cells was then determined via flow cytometry by first gating on the DiD$^-$ cell population. (B) Representative data showing percent GFP expression on CD4$^+$ T cells with or without 5 h of NK cell coculture in the presence of isotype Abs or ICAM-1 blocking Abs. (C) For both antibody treatments, the percent specific lysis of infected CD4$^+$ T cells was calculated by dividing the decrease in percent GFP$^+$ CD4$^+$ T cells resulting from NK cell coculture [(percent GFP$^+$ of DiD$^-$ cells$_{\text{no NK cell coculture}}$) − (percent GFP$^+$ of DiD$^-$ cells$_{\text{NK cell coculture}}$)] by the percent GFP$^+$ CD4$^+$ T cells without NK cell coculture [(percent GFP$^+$ of DiD$^-$ cells$_{\text{no NK cell coculture}}$) × 100]. (D) Compiled data expressed relative to WT-infected, ISO-treated samples ($n \geq 4$). The error bars represent SEM. *, $P \leq 0.05$; N.S., nonsignificant.

experiments using ΔVpu HIV-1 infection and Vpu-encoding lentiviral vector transduction in order to assess the role of Vpu in the downregulation of specific candidates. Our study, in contrast, employed a Vpu-inducible Jurkat cell line to directly assess the role of Vpu. Despite these differences in the experimental approaches, several putative targets for HIV-1-mediated downregulation were identified in both studies, including multiple members of the ICAM family (see Table S1 in the supplemental material).

Previously, Haller and colleagues employed a flow cytometry-based screening assay to uncover novel targets of Vpu-mediated downregulation (53). This group transiently transfected A3.01 lymphocytes to express Vpu and then observed the effects of the viral protein using a commercially available Ab screening panel comprised of 242

distinct Abs. Interestingly, this directed screening assay also identified ICAM-2 as a candidate for Vpu-mediated downregulation. Furthermore, the study also identified numerous members of the tetraspanin family of proteins (CD37, CD53, CD63, CD81, and CD151) as Vpu targets, a finding that was later supported by the Matheson et al. study. In contrast, Haller et al. failed to observe Vpu-mediated changes in many putative targets identified using proteomic-based screening methods (ICAM-3 [CD50], IAP [CD47], SPN [CD43], and MIC2 [CD99]). These discrepancies may be the result of the expression system used (transient expression versus stable expression versus infection), differences in model cell lines, or variations in the sensitivity of the screening assays.

Our study has ultimately led to the identification and validation of the adhesion molecules ICAM-1 and ICAM-3 as surface molecules downmodulated by Vpu (Fig. 1 and 2). While ICAM-2 is generally believed to be the most relevant for endothelial cell function (32, 33), ICAM-1 and ICAM-3 expressed on leukocytes are important components of the highly organized and stable cell-to-cell contacts termed IS structures. ICAM-3 is expressed constitutively at high levels, while ICAM-1 is generally expressed at low levels but can be dramatically upregulated in response to numerous stimuli, including cytokines, hormones, infections, and physical stressors (54), as well as, importantly, T cell activation and direct T cell receptor (TCR) stimulation (55). ICAM-3 binding has been shown to induce enlargement of cell-to-cell contacts through increased actin polymerization, while ICAM-1 does not (for a review, see reference 32). Rather, ICAM-1 supports more prolonged and stable conjugations (56). These observations have led to a model whereby ICAM-3 is responsible for less specific cell-to-cell interactions that promote the expansion of the initial contact interface, while ICAM-1 binding cements the strong, stable attachment needed for IS formation.

We confirmed the previous *in vivo* observation that ICAM-1 is upregulated at the transcriptional level in the context of HIV-1 infection (36) and further showed that Vpu counterbalances this upregulation by downregulating ICAM-1 posttranscriptionally (Fig. 2 and 3). Vpu-mediated downregulation results in an approximately 2-fold decrease in the relative expression of surface ICAM-1 on HIV-1-infected cells (Fig. 2), similar to what has been reported for BST2 in this context (57, 58). This effect requires the presence of a dual-serine motif at amino acids S52/S56 and an intact TMD (Fig. 2 and 4) and is conserved among primary Vpu variants (Fig. 4).

Importantly, we showed that ICAM-1 downmodulation decreases the ability of NK cells to target infected $CD4^+$ T cells for deletion (Fig. 8 and 9) while at the same time decreasing HIV-1 particle infectivity (Fig. 7). In contrast, ICAM-3 was packaged into HIV-1 virions only at very low levels and did not significantly affect infectivity, confirming previous results (49). Furthermore, whereas ICAM-1 blocking Abs produced a profound loss of conjugate formation between NK cells and infected $CD4^+$ T cells in all contexts, blocking ICAM-3 resulted in only a slight decrease in conjugate formation, and only at high ICAM-3 surface levels resulting from the absence of Vpu. Collectively, these observations suggest that ICAM-1 plays a more significant role in both HIV-1 virion infectivity and formation of IS structures between infected T cells and NK cells than the related ICAM-3 molecule.

Mechanistically, we provided evidence that Vpu interacts with ICAM-1 via its TMD and accelerates its degradation via a proteasome-dependent process (Fig. 5) that relies on the recruitment of β-TrCP-1 (Fig. 6), likely prior to ICAM-1 maturation in the ER (Fig. 5). Interestingly, although both surface downregulation and degradation of ICAM-1 are dependent on the S52/S56 motif and TMD of Vpu, β-TrCP-1 is not required for ICAM-1 surface downregulation (Fig. 6).

The data presented here, taken as a whole, suggest a model whereby ICAM-1 transcripts are increased in response to viral infection, while Vpu mitigates this upregulation by intercepting immature ICAM-1 and promoting its proteasome degradation through ubiquitination by the $SCF^{\beta\text{-TrCP-1}}$ E3 ubiquitin ligase complex. In the absence of β-TrCP-1, however, Vpu is still able to sequester ICAM-1 intracellularly in an S52/S56-dependent manner, resulting in decreased ICAM-1 surface expression without whole-cell protein loss. This at first appears to be paradoxical, as the S52/S56 motif of

Vpu acts primarily to recruit β-TrCP and its accompanying ubiquitination machinery. Deletion of the S52/S56 motif would therefore be expected to phenocopy β-TrCP knockdown in all respects. Recently however, it has been shown that the phosphorylation of S52/S56 also regulates other functions of Vpu. For example, Vpu S52/S56 phosphorylation also allows the recruitment of clathrin adaptor proteins 1 and 2 (AP-1 and AP-2) to the cytosolic tail of Vpu, allowing Vpu to link its targets to clathrin-dependent endocytic trafficking machinery independently of β-TrCP recruitment (42, 43). Indeed, somewhat analogous to our ICAM-1 findings, S52/S56-mediated downregulation of BST2 (through recruitment of AP-1) and S52/S56-mediated BST2 lysosomal degradation (through recruitment of $SCF^{\beta\text{-TrCP}}$) have already been shown to be separable phenomena (43). The most parsimonious hypothesis is that Vpu interacts with immature ICAM-1 directly in the ER or early *cis*-Golgi, preventing its transition to the cell surface through a mechanism requiring the S52/S56 motif (yet independent of β-TrCP). This pool of ICAM-1 becomes susceptible to Vpu-mediated proteasomal degradation through S52/S56-mediated recruitment of β-TrCP-1. One way Vpu could retain ICAM-1 within the cell is by directly inhibiting ICAM-1 glycosylation. Indeed, ICAM-1 has been shown to be retained in the ER when glycosylation is prevented (59). In addition, Vpu has been shown to prevent the glycosylation of both NTB-A, resulting in its lowered surface expression (60), and BST2, potentially inhibiting its translocation into the ER (61). Alternatively, the possibility that Vpu can interact with ICAM-1 in the ER or *cis*-Golgi to induce its degradation via β-TrCP, as well as interact with the protein at other locations within the cell to induce β-TrCP-1-independent sequestration, cannot be excluded.

The ability of Vpu to prevent ICAM-1-mediated NK cell/$CD4^+$ T cell conjugation suggests Vpu disrupts the formation of IS structures. Interestingly, Vpu is not the first viral protein demonstrated to decrease ICAM-1 levels to promote evasion of cell-mediated immunity. Indeed, the p12(I) protein from human T-cell lymphotropic virus type 1 (HTLV-1) also decreases ICAM-1 surface expression on infected $CD4^+$ T cells, resulting in lowered NK cell conjugation (62). In addition, the membrane-associated E3 ubiquitin ligase K5 and K3 proteins from gammaherpesviruses also target ICAM-1 for degradation to similar effect (63).

ICAM-1 is known to localize to HIV assembly sites (64), and a highly developed body of work describing the infectivity-enhancing incorporation of ICAM-1 into HIV-1 particles has been published (44). The observation that Vpu-mediated ICAM-1 downregulation results in its decreased incorporation into virions and accompanying lower viral infectivity was therefore not unexpected. It is noteworthy that ICAM-1 also plays a major role in the formation of direct contacts between infected cells and uninfected target cells resembling IS structures, referred to as virological synapses (VS) (65). VS structures promote direct cell-to-cell transmission of HIV, resulting in more efficient viral dissemination than is achieved with cell-free virions (66), as well as helping to bypass antibody defenses (67) and encouraging inflammation-induced apoptosis (termed pyroptosis) of nonpermissive $CD4^+$ target T cells (68).

Vpu-mediated ICAM-1 downregulation may therefore represent an evolutionary compromise on the part of the virus, allowing the evasion of cell-mediated immunity at the cost of decreased viral infectivity and VS-mediated spread. Consistent with this idea, Vpu has been shown to inhibit HIV-1 cell-to-cell transmission in both BST2-expressing (69) and BST2-deficient (70) cells and is selected against during long-term *in vitro* culture, perhaps resulting in enhanced cell-to-cell transmission (71). A similar evolutionary compromise has been proposed for the Vpu-targeted tetraspanin molecules (27). Tetraspanins are surface membrane proteins that have been reported to benefit HIV-1 by preventing the cell-to-cell fusion events that lead to the formation of syncytia (72) yet hinder HIV-1 by decreasing infectivity when packaged into virions (73). Interestingly, tetraspanin molecules are known to organize into membrane microstructures referred to as tetraspanin-enriched microdomains (TEMs), which specifically incorporate ICAM-1 (74) and localize to both IS and VS structures, where they modulate HIV-1 cell-to-cell spread (75, 76). Although, unlike ICAM-1, Vpu-mediated downregula-

tion of tetraspanins does not require the S52/S56 dual-serine motif, the potential for at least a partially shared mechanism warrants further study.

Given the ubiquitous role of ICAM-1 in the proper formation of IS/VS structures, the negative effects of Vpu-mediated ICAM-1 downregulation likely extend well beyond NK cell immune evasion. For example, antigen-presenting cells, such as macrophages, also rely on IS structures to identify HIV-infected T cells (77). Furthermore, $CD8^+$ T cell-mediated immunity, a dominant contributor to the control of HIV-1 viremia, also depends on ICAM-enhanced IS structures for the identification and destruction of infected cells (78). Clearly, a fuller understanding of the immunological consequences of Vpu-mediated ICAM downregulation remains an important research goal that warrants further investigation.

MATERIALS AND METHODS

Antibodies and reagents. For flow cytometry, anti-ICAM-1–allophycocyanin (APC) (HA58), anti-ICAM-3-APC (CBR-IC3/1), and anti-CD45-phycoerythrin (PE)-Cy7 (H130) Abs were purchased from BioLegend (San Diego, CA). Anti-TfR-APC (M-A712) Abs were obtained from BD Bioscience (San Jose, CA), while goat anti-rabbit–Alexa Fluor 633 (A633) Abs were purchased from Life Technologies (Thermo Fisher, Carlsbad, CA). Rabbit anti-BST2 serum was described previously (19). For Western blot experiments, rabbit anti-ICAM-1 (sc-7891), goat anti-calnexin (sc-6465), rabbit anti-Eps15 (sc-534), and rabbit anti-CD4 (sc-7219) were obtained from Santa Cruz (Dallas, TX); rabbit anti-ICAM-3 (AF813) was purchased from R&D Systems (Minneapolis, MN), mouse monoclonal anti-TfR (BD 612124) from BD Bioscience, rabbit anti-histone H3 (ab1794) from Abcam (Toronto, Canada), sheep anti-TGN46 (AHP500G) from AbD Serotec (Raleigh, NC), rabbit anti-AU1 (LS-C83247) from LSBio (Seattle, WA), rabbit anti-glyceraldehyde-3-phosphate dehydrogenase (GAPDH) (poly6314) from BioLegend, and mouse monoclonal anti-GFP from Roche (Mississauga, Canada). Anti-actin rabbit serum (A2668) was purchased from Sigma-Aldrich (St. Louis, MO). Rabbit anti-Vpu, mouse anti-p24, and anti-gp120 sera were described previously (79, 80). For coimmunoprecipitation (co-IP) experiments, goat polyclonal anti-ICAM-1 Abs (BBA17) were purchased from R&D Systems. For NK cell blocking experiments, mouse monoclonal IgG1 anti-ICAM-1 Abs (clone 15.2) and anti-ICAM-3 Abs (clone CBR-IC3/1) were purchased from AbD Serotec and BioLegend, respectively, while the mouse IgG1 Abs (P3.6.2.8.1) used as an isotype control were obtained from eBioscience (San Diego, CA).

Expre^{35}S^{35}S labeling reagent was purchased from Perkin Elmer. Heavy-labeled L-arginine-HCl ($^{13}C_6H_{14}{}^{15}N_4O_2$:HCl) and L-lysine-HCl ($^{13}C_6H_{14}{}^{15}N_2O_2$:2HCl) were obtained from Cambridge Isotope Laboratories (Andover, MA), whereas natural L-arginine-HCl, L-lysine-HCl, and L-leucine-HCl were purchased from Sigma-Aldrich. Raltegravir and interleukin 2 (IL-2) were obtained through the NIH AIDS Reagent Program, Division of AIDS, NIAID, NIH, from Merck (Kenilworth, NJ), and from Maurice Gately (Roche).

Plasmids. A pNL4.3 proviral construct coding for a full-length B clade HIV-1 group M in which *nef* is followed by an internal ribosome entry site (IRES) that allows expression of GFP (pNL4.3-GFP) and isogenic variants thereof have been described previously (79, 81, 82). The plasmids encoding Vpu variants with a disrupted hydrophobic face within the TMD at amino acids A10, A14, A18 (A10/A14/A18L) and the S52/S56 motif (S52/S56D) were generated by site-directed mutagenesis of the original pNL4.3-GFP. pCGCG-Vpu-IRES-GFP plasmids expressing a bicistronic mRNA encoding group M Vpu variants with an AU1 tag at their C termini and GFP from an IRES element were provided by Frank Kirchhoff (39). Mutant variants of the pCGCG NL4.3 Vpu plasmids were generated by site-directed mutagenesis. The cytomegalovirus (CMV) early promoter-based plasmids (svCMV) expressing either WT or mutant Vpu proteins have been described previously (83, 84). The pLenti-CMV/TO_Puro_DEST and pLenti-CMV-TetR plasmids were acquired from Addgene (Eric Campeau), and a coding sequence expressing VpuGFP was inserted into pLenti-CMV/TO_Puro_DEST using standard molecular techniques. The lentiviral psPAX2 packaging vector and the pCD1.8 plasmid encoding ICAM-1 (pICAM-1) were obtained through Addgene from Didier Trono and Timothy Springer, respectively. The ICAM-3-expressing pCMV/hygro plasmid (pICAM-3) was purchased from Sino Biological (Beijing, China). The pVSVg vector encoding VSV-G has been described previously (79). The pCMV6-XL5 plasmid encoding TfR (pTfR) was purchased from OriGene.

Cell lines and tissue culture. Lymphocytic cell lines were cultured in RPMI 1640 medium (Wisent) supplemented with 10% fetal calf serum (FCS), 100 U/ml penicillin, and 100 μg/ml streptomycin (RPMI-10). HeLa cells and HEK 293T cells were cultured in Dulbecco's modified Eagle's medium (DMEM) (Wisent) supplemented with 10% FCS (DMEM-10). Primary $CD4^+$ T cells were maintained at 1×10^6 cells/ml in RPMI-10 supplemented with 100 U/ml IL-2. Primary $CD56^+$ NK cells were maintained at 1×10^6 cells/ml in RPMI-10 supplemented with 500 U/ml IL-2.

Jurkat^{tetR}VpuGFP cells were generated by transducing Jurkat E6.1 cells with lentiviral vectors coding for VpuGFP expressed from a CMV early promoter under the control of the tetracycline (Tet) response element, followed by a second round of lentiviral transduction with vectors encoding the TetR repressor protein under the control of the CMV promoter. Gene selection was carried out through the sequential addition of 1 μg/ml of puromycin (Sigma-Aldrich) and 100 μg/ml of blasticidin (Sigma-Aldrich) to cell cultures to select for VpuGFP and TetR, respectively.

HeLa cells stably expressing shRNA against β-TrCP-1, β-TrCP-2, or a nontargeting control from a bicistronic mRNA that also produces GFP were generated by lentiviral transduction. Selection was carried

out by supplementing the cell cultures with 1 μg/ml of puromycin, followed by FACS for GFP^{high} cells. CEM cells resistant to NK cell-mediated lysis (CEM NK^r CCR5$^+$) were obtained from the NIH AIDS Reagent Program (John Moore and Catherine Spenlehauer) and altered to stably express shRNA against BST2 (CEM-shBST2) by lentiviral transduction followed by puromycin selection (85).

Jurkat-1G5 cells and HeLa Tzm-bl expressing luciferase under the control of the HIV-1 LTR were obtained from the NIH AIDS Reagent Program (Estuardo Aguilar-Cordova and John Belmont [Jurkat-1G5]; John C. Kappes, Xiaoyun Wu, and Tranzyme Inc. [Hela Tzm-bl]). SupT1 cells and CEM NK^r CCR5$^+$ cells expressing luciferase under the control of the HIV-1 LTR (CEM-luc) were also obtained from the NIH AIDS Reagent Program (Dharam Ablashi [SupT1]; John Moore and Catherine Spenlehauer [CEM-luc]). The NK-like YTS cells were a generous gift from André Veillette (Institut de Recherches Cliniques de Montréal [IRCM]).

Virus and lentiviral vector production. HEK 293T cells were transfected with proviral plasmids using a standard calcium phosphate method as described previously (79). For HIV-1 production, cells were transfected with pNL4.3-GFP or isogenic variants thereof. To pseudotype certain virus preparations, the pVSVg plasmid was cotransfected. For lentiviral production, cells were transfected with pVSVg, psPAX2, and pLenti-CMV/TO_Puro_DEST encoding either VpuGFP or pLenti-CMV-TetR, as previously described (79). Virus stocks were quantified using a standard MAGI assay as described previously (79).

SILAC, plasma membrane isolation, and mass spectrometry. For a minimum of six doubling times, Jurkat^{tetR}VpuGFP cells were grown in leucine-free, lysine-free, arginine-free, and phenol red-free RPMI 1640 media (Sigma-Aldrich) supplemented with 50 μg/ml L-lysine, penicillin-streptomycin (P/S), and 10% dialyzed FCS, with either natural or heavy-labeled L-arginine and L-lysine added at 200 μM and 335 μM, respectively. After label incorporation, 7×10^7 cells were cultured at 1×10^6 cells/ml and either treated with Dox (Sigma-Aldrich) at 7 μg/ml or left untreated for 36 h. The treated and untreated cells were then mixed together at a 1:1 ratio, and PMs were isolated using cationic colloidal silica beads as described previously (28). Briefly, cells were coated with Ludox colloidal silica beads (Sigma-Aldrich) and then suspended in lysis buffer (phosphate-buffered saline [PBS] with 0.1% Triton X-100, 0.1% [mass/vol] SDS supplemented with fresh Complete protease inhibitor [Roche] and 10 μg/ml DNase [Roche]) and lysed by sonication on ice with 2 30-s pulses at 70% amperage using a Branson Ultrasonics (Danbury, CT) Sonifier 450 sonicator. Membrane proteins were pelleted by zonal centrifugation over a 10% to 60% laddered sucrose gradient and purified as described previously (28). Proteins were then precipitated using standard trichloroacetic acid (TCA) precipitation and sent to the IRCM Proteomics discovery platform for MS analysis. Proteins were identified and quantified using the MaxQuant SILAC computer program (version 1.5.3.30; Max Plank Institute of Biochemistry [http://www.coxdocs.org/doku.php?id=maxquant:start]).

Primary lymphocyte isolation, culture, and infection. Peripheral blood samples were obtained from healthy adult donors who gave written informed consent in accordance with the Declaration of Helsinki under research protocols approved by the research ethics review board of the IRCM. Peripheral blood mononuclear cells (PBMCs) were isolated by Ficoll Paque (Roche) density centrifugation, and primary CD4$^+$ T cells and NK cells were isolated, activated, and cultured as described previously (86), with the exception that NK cells were maintained in the presence of 500 U/ml of IL-2.

CD4$^+$ T cells were infected with GFP-marked WT NL4.3 HIV-1 or isogenic Vpu variants thereof at a multiplicity of infection (MOI) of 0.5. Surface expression of various molecules was measured by flow cytometry 48 h postinfection using a Beckman Coulter (Mississauga, Canada) cyan ADP flow cytometer.

HeLa cell infection. HeLa cells were infected with VSV-G$^+$ GFP-marked WT or Vpu-deficient (ΔVpu) NL4.3 HIV-1 at an MOI of 5 for 48 h. Aliquots of the infected samples were lysed in radioimmunoprecipitation assay (RIPA) buffer and analyzed by Western blotting, as described previously (83). In parallel, RNA was isolated from infected HeLa cells using the RNeasy plus kit (Qiagen, Toronto, Canada), and cDNA was generated by RT-PCR using a Superscript II kit (Invitrogen, Thermo Fisher). qPCR was carried out using SYBR green (Thermo Fisher) on a Viaa-7 PCR System thermocycler (Thermo Fisher). Transcripts were quantified using the $2^{\Delta\Delta CT}$ method. The qPCR primers were as follows: ICAM-1 forward (Fwd), 5′-CCTC AGCACGTACCTCTATAAC-3′; ICAM-1 reverse (Rev), 5′-GGCTTGTGTGTTCGGTTTC-3′; BST2 Fwd, 5′-CAGAA GGGCTTTCAGGATG-3′; BST2 Rev, 5′-TTTGTCCTTGGGCCTTCTC-3′; GAPDH Fwd, 5′-GGTGTGAACCATGAG AAGTATGA-3′; GAPDH Rev, 5′-GAGTCCTTCCACGATACCAAAG-3′; β-TrCP-1 Fwd, 5′-TGGCTCATCTGACAA CACTATC-3′; β-TrCP-1 Rev, 5′-CGAATACAACGCACCAATTCC-3′; β-TrCP-2 Fwd, 5′-TTCGGCTCCAGTTTGAT GAG-3′; β-TrCP-2 Rev, 5′-CACTGGGAGGCACATTTAAGA-3′.

HeLa and HEK 293 T cell transfection. HeLa and HEK 293T cells were transfected with the described plasmid vectors using Lipofectamine 2000 (Invitrogen) 24 or 48 h prior to further experimentation.

Metabolic labeling, pulse-chase, and immunoprecipitation. HeLa cells were washed two times in methionine- and cysteine-free DMEM (Wisent) supplemented with P/S and 10% dialyzed FCS, subsequently starved for 45 min in this medium in the presence or absence of CMA (Tocris Bioscience, Minneapolis, MN) or MG132 (Calbiochem, Etobicoke, Canada), and then pulsed for 1 h by adding ^{35}S-labeled methionine and cysteine Expre^{35}S^{35}S (Perkin Elmer, Waltham, MA) at 400 μCi/ml. The cells were then washed two times in DMEM-10 and lysed at specific time points in RIPA buffer. ICAM-1 was immunoprecipitated using an excess of goat anti-ICAM-1 Abs, and radiolabeled immunoprecipitates were separated via SDS-PAGE and analyzed using a Storm 860 molecular imager (Molecular Dynamics, GE Healthcare) as described previously (83).

Coimmunoprecipitation. HeLa cells were infected with WT or ΔVpu HIV-1 or HIV-1 encoding a Vpu mutant lacking the conserved transmembrane triple-alanine motif (A10/A14/A18L Vpu) as described above and then lysed in CHAPS buffer (50 mM Tris, 100 mM NaCl, 0.5% [wt/vol] CHAPS {3-[(3-cholamidopropyl)-dimethylammonio]-1-propanesulfonate}, 5 mM EDTA, pH 7.2, supplemented with

fresh 1× Complete protease inhibitor). Lysates were precleared by incubation with 30 μl of CHAPS buffer-washed protein G agarose beads (Thermo Fisher) for 1 h at 4°C. The lysates were then incubated with goat anti-ICAM-1 Abs 4 to 6 h prior to the overnight addition of 40 μl of protein G beads. The beads were washed four times with complete CHAPS buffer and then analyzed by Western blotting, as described above.

Infectivity assay. SupT1 and CEM-shBST2 cells were infected with WT or ΔVpu NL4.3 HIV-1 at an MOI of 0.5. HEK 293T cells were transfected with GFP-marked WT or ΔVpu HIV-1 or HIV-1 encoding a Vpu mutant lacking the dual-serine motif (S52/S56D Vpu) pNL4.3 proviruses and simultaneously cotransfected with either pICAM-1, pICAM-3, or pTfR expressor plasmids. Forty-eight hours postinfection (SupT1 and CEM-shBST2) or posttransfection (HEK 293T), viruses were isolated by ultracentrifugation, as described previously (79), and normalized for p24 expression using an anti-p24 ELISA (XpressBio, Frederick, MD). Jurkat-1G5, HeLa Tzm-bl, or CEM-luc cells, which express luciferase under the control of the HIV-1 LTR promoter (47, 48, 87), were infected with virus at 50 pg of p24 per 1×10^5 cells and investigated for luciferase production 48 h later using a luciferase assay system kit (Promega, Madison, WI).

CD4$^+$ T cell-NK cell conjugation assays. Ten million isolated CD4$^+$ T cells per condition were infected with VSV-G$^+$ GFP-marked WT, ΔVpu, or S52/S56D Vpu NL4.3 at an MOI of 1 via spin infection. Forty-eight hours postinfection, GFP$^+$ CD4$^+$ T cells were enriched to greater than 99% purity by FACS. Autologous NK cells were labeled with eFluor 670 dye (eBioscience). Infected CD4$^+$ T cells were mixed with autologous dye-labeled NK cells at an E:T ratio of 1:1 or 2.5:1 and placed at 37°C for 10 min. The CD4$^+$ T cell-NK cell conjugates were fixed by the addition of equal parts (vol/vol) of 4% PFA (Sigma-Aldrich) in PBS, and the conjugates were analyzed by flow cytometry as described previously (51).

For anti-ICAM-1 and anti-ICAM-3 blocking experiments, primary CD4$^+$ T cells were pretreated with either anti-ICAM-1 or anti-ICAM-3 blocking Abs or an isotype control at 10 μg/ml for 1 h at 4°C prior to mixing with NK-like YTS cells at an E:T ratio of 3:1 for 15 min at 37°C. The cells were then fixed in 2% PFA, and flow cytometry was carried out as described above.

NK cell-specific lysis assay. Primary CD4$^+$ T cells were infected with VSV-G$^+$ GFP-marked WT, ΔVpu, or S52/S56D Vpu NL4.3 at an MOI of 1. Autologous NK cells were labeled with Vybrant DiD dye (ThermoFisher). Forty-eight hours postinfection, the cells were pretreated with mouse anti-ICAM-1 blocking Abs or isotype control Abs at 10 μg/ml for 1 h at 4°C and then mixed or not with autologous NK cells at an E:T ratio of 3:1 for 5 h in the presence of 200 U/ml of IL-2. The cells were then fixed in 2% PFA and analyzed by flow cytometry. The percent specific lysis of GFP-marked infected cells was calculated by enumerating the change in DiD$^-$ GFP$^+$ cell numbers in the presence or absence of NK cells: (100 × [percent GFP$^+$ of DiD$^-$ cells without NK cell coculture] − [percent GFP$^+$ of DiD$^-$ cells with 5 h of NK cell coculture]/[percent GFP$^+$ of DiD$^-$ cells without NK cell coculture]).

Statistical analysis. Student's *t* tests were used to compare individual conditions for statistically significant differences.

SUPPLEMENTAL MATERIAL

Supplemental material for this article may be found at https://doi.org/10.1128/JVI.02442-16.

TABLE 1, PDF file, 0.1 MB.

ACKNOWLEDGMENTS

We thank Catherine Paquay for the shβ-TrCP-expressing HeLa cells, as well as the Proteomics, Cytometry, and Molecular Biology platforms of the IRCM for their services and expertise. We thank the NIH AIDS Reagent Program for providing IL-2 (Maurice Gately), Jurkat-1G5 cells (Estuardo Aguilar-Cordova and John Belmont), SupT1 cells (Dharam Ablashi), CEM NK^r CCR5$^+$ luciferase$^{+/-}$ cells (John Moore and Catherine Spenlehauer), and HeLa Tzm-bl cells (John C. Kappes, Xiaoyun Wu, and Tranzyme Inc.). We thank Didier Trono and Timothy Springer for contributing psPAX2 and ICAM-1-expressing plasmids to the Addgene repository, respectively. We thank Frank Kirchhoff for providing primary Vpu variant-expressing pCGCG plasmids and André Veillette for providing YTS cells as well as the experimental expertise to perform the CD4$^+$ T cell-NK cell conjugation assay. We thank Mariana Bego, Édouard Bérubé-Côté, and Mildred Delaleau for help generating and characterizing Jurkat^{TetR}VpuGFP cells.

This work was supported by Canadian Institutes of Health Research (CIHR) grant MOP-111226 and by Canadian HIV Cure Enterprise grant HIG-133050 from the CIHR partnership with CANFAR and IAS to E.A.C. E.A.C. is the recipient of the IRCM-Université de Montréal Chair of Excellence in HIV Research.

REFERENCES

1. Cohen EA, Terwilliger EF, Sodroski JG, Haseltine WA. 1988. Identification of a protein encoded by the vpu gene of HIV-1. Nature 334:532–534. https://doi.org/10.1038/334532a0.
2. Strebel K, Klimkait T, Martin MA. 1988. A novel gene of HIV-1, vpu, and its 16-kilodalton product. Science 241:1221–1223. https://doi.org/10.1126/science.3261888.
3. Salazar-Gonzalez JF, Salazar MG, Keele BF, Learn GH, Giorgi EE, Li H, Decker JM, Wang S, Baalwa J, Kraus MH, Parrish NF, Shaw KS, Guffey MB, Bar KJ, Davis KL, Ochsenbauer-Jambor C, Kappes JC, Saag MS, Cohen MS, Mulenga J, Derdeyn CA, Allen S, Hunter E, Markowitz M, Hraber P, Perelson AS, Bhattacharya T, Haynes BF, Korber BT, Hahn BH, Shaw GM. 2009. Genetic identity, biological phenotype, and evolutionary pathways of transmitted/founder viruses in acute and early HIV-1 infection. J Exp Med 206:1273–1289. https://doi.org/10.1084/jem.20090378.
4. Dave VP, Hajjar F, Dieng MM, Haddad E, Cohen EA. 2013. Efficient BST2 antagonism by Vpu is critical for early HIV-1 dissemination in humanized mice. Retrovirology 10:128. https://doi.org/10.1186/1742-4690-10-128.
5. Sato K, Misawa N, Fukuhara M, Iwami S, An DS, Ito M, Koyanagi Y. 2012. Vpu augments the initial burst phase of HIV-1 propagation and downregulates BST2 and CD4 in humanized mice. J Virol 86:5000–5013. https://doi.org/10.1128/JVI.07062-11.
6. Margottin F, Bour SP, Durand H, Selig L, Benichou S, Richard V, Thomas D, Strebel K, Benarous R. 1998. A novel human WD protein, h-beta TrCp, that interacts with HIV-1 Vpu connects CD4 to the ER degradation pathway through an F-box motif. Mol Cell 1:565–574. https://doi.org/10.1016/S1097-2765(00)80056-8.
7. Sugden SM, Bego MG, Pham TN, Cohen EA. 2016. Remodeling of the host cell plasma membrane by HIV-1 Nef and Vpu: a strategy to ensure viral fitness and persistence. Viruses 8:67. https://doi.org/10.3390/v8030067.
8. Willey RL, Maldarelli F, Martin MA, Strebel K. 1992. Human immunodeficiency virus type 1 Vpu protein induces rapid degradation of CD4. J Virol 66:7193–7200.
9. Neil SJ, Zang T, Bieniasz PD. 2008. Tetherin inhibits retrovirus release and is antagonized by HIV-1 Vpu. Nature 451:425–430. https://doi.org/10.1038/nature06553.
10. Van Damme N, Goff D, Katsura C, Jorgenson RL, Mitchell R, Johnson MC, Stephens EB, Guatelli J. 2008. The interferon-induced protein BST-2 restricts HIV-1 release and is downregulated from the cell surface by the viral Vpu protein. Cell Host Microbe 3:245–252. https://doi.org/10.1016/j.chom.2008.03.001.
11. Wildum S, Schindler M, Munch J, Kirchhoff F. 2006. Contribution of Vpu, Env, and Nef to CD4 down-modulation and resistance of human immunodeficiency virus type 1-infected T cells to superinfection. J Virol 80:8047–8059. https://doi.org/10.1128/JVI.00252-06.
12. Willey RL, Maldarelli F, Martin MA, Strebel K. 1992. Human immunodeficiency virus type 1 Vpu protein regulates the formation of intracellular gp160-CD4 complexes. J Virol 66:226–234.
13. Lama J, Mangasarian A, Trono D. 1999. Cell-surface expression of CD4 reduces HIV-1 infectivity by blocking Env incorporation in a Nef- and Vpu-inhibitable manner. Curr Biol 9:622–631. https://doi.org/10.1016/S0960-9822(99)80284-X.
14. Pham TN, Lukhele S, Hajjar F, Routy JP, Cohen EA. 2014. HIV Nef and Vpu protect HIV-infected CD4$^+$ T cells from antibody-mediated cell lysis through down-modulation of CD4 and BST2. Retrovirology 11:15. https://doi.org/10.1186/1742-4690-11-15.
15. Veillette M, Coutu M, Richard J, Batraville LA, Dagher O, Bernard N, Tremblay C, Kaufmann DE, Roger M, Finzi A. 2015. The HIV-1 gp120 CD4-bound conformation is preferentially targeted by antibody-dependent cellular cytotoxicity-mediating antibodies in sera from HIV-1-infected individuals. J Virol 89:545–551. https://doi.org/10.1128/JVI.02868-14.
16. McNatt MW, Zang T, Bieniasz PD. 2013. Vpu binds directly to tetherin and displaces it from nascent virions. PLoS Pathog 9:e1003299. https://doi.org/10.1371/journal.ppat.1003299.
17. Mitchell RS, Katsura C, Skasko MA, Fitzpatrick K, Lau D, Ruiz A, Stephens EB, Margottin-Goguet F, Benarous R, Guatelli JC. 2009. Vpu antagonizes BST-2-mediated restriction of HIV-1 release via beta-TrCP and endo-lysosomal trafficking. PLoS Pathog 5:e1000450. https://doi.org/10.1371/journal.ppat.1000450.
18. Tokarev AA, Munguia J, Guatelli JC. 2011. Serine-threonine ubiquitination mediates downregulation of BST-2/tetherin and relief of restricted virion release by HIV-1 Vpu. J Virol 85:51–63. https://doi.org/10.1128/JVI.01795-10.
19. Dube M, Roy BB, Guiot-Guillain P, Binette J, Mercier J, Chiasson A, Cohen EA. 2010. Antagonism of tetherin restriction of HIV-1 release by Vpu involves binding and sequestration of the restriction factor in a perinuclear compartment. PLoS Pathog 6:e1000856. https://doi.org/10.1371/journal.ppat.1000856.
20. Apps R, Del Prete GQ, Chatterjee P, Lara A, Brumme ZL, Brockman MA, Neil S, Pickering S, Schneider DK, Piechocka-Trocha A, Walker BD, Thomas R, Shaw GM, Hahn BH, Keele BF, Lifson JD, Carrington M. 2016. HIV-1 Vpu mediates HLA-C downregulation. Cell Host Microbe 19:686–695. https://doi.org/10.1016/j.chom.2016.04.005.
21. Shah AH, Sowrirajan B, Davis ZB, Ward JP, Campbell EM, Planelles V, Barker E. 2010. Degranulation of natural killer cells following interaction with HIV-1-infected cells is hindered by downmodulation of NTB-A by Vpu. Cell Host Microbe 8:397–409. https://doi.org/10.1016/j.chom.2010.10.008.
22. Moll M, Andersson SK, Smed-Sorensen A, Sandberg JK. 2010. Inhibition of lipid antigen presentation in dendritic cells by HIV-1 Vpu interference with CD1d recycling from endosomal compartments. Blood 116:1876–1884. https://doi.org/10.1182/blood-2009-09-243667.
23. Matusali G, Potesta M, Santoni A, Cerboni C, Doria M. 2012. The human immunodeficiency virus type 1 Nef and Vpu proteins downregulate the natural killer cell-activating ligand PVR. J Virol 86:4496–4504. https://doi.org/10.1128/JVI.05788-11.
24. Ramirez PW, Famiglietti M, Sowrirajan B, DePaula-Silva AB, Rodesch C, Barker E, Bosque A, Planelles V. 2014. Downmodulation of CCR7 by HIV-1 Vpu results in impaired migration and chemotactic signaling within CD4(+) T cells. Cell Rep 7:2019–2030. https://doi.org/10.1016/j.celrep.2014.05.015.
25. Vassena L, Giuliani E, Koppensteiner H, Bolduan S, Schindler M, Doria M. 2015. HIV-1 Nef and Vpu interfere with L-selectin (CD62L) cell surface expression to inhibit adhesion and signaling in infected CD4$^+$ T lymphocytes. J Virol 89:5687–5700. https://doi.org/10.1128/JVI.00611-15.
26. Matheson NJ, Sumner J, Wals K, Rapiteanu R, Weekes MP, Vigan R, Weinelt J, Schindler M, Antrobus R, Costa AS, Frezza C, Clish CB, Neil SJ, Lehner PJ. 2015. Cell surface proteomic map of HIV infection reveals antagonism of amino acid metabolism by Vpu and Nef. Cell Host Microbe 18:409–423. https://doi.org/10.1016/j.chom.2015.09.003.
27. Lambele M, Koppensteiner H, Symeonides M, Roy NH, Chan J, Schindler M, Thali M. 2015. Vpu is the main determinant for tetraspanin down-regulation in HIV-1-infected cells. J Virol 89:3247–3255. https://doi.org/10.1128/JVI.03719-14.
28. Chaney LK, Jacobson BS. 1983. Coating cells with colloidal silica for high yield isolation of plasma membrane sheets and identification of transmembrane proteins. J Biol Chem 258:10062–10072.
29. Chen X, Wei S, Ji Y, Guo X, Yang F. 2015. Quantitative proteomics using SILAC: principles, applications, and developments. Proteomics 15:3175–3192. https://doi.org/10.1002/pmic.201500108.
30. Cervantes-Acosta G, Cohen EA, Lemay G. 2001. Human Jurkat lymphocytes clones differ in their capacity to support productive human immunodeficiency virus type 1 multiplication. J Virol Methods 92:207–213. https://doi.org/10.1016/S0166-0934(00)00289-5.
31. Kinet S, Bernard F, Mongellaz C, Perreau M, Goldman FD, Taylor N. 2002. gp120-mediated induction of the MAPK cascade is dependent on the activation state of CD4(+) lymphocytes. Blood 100:2546–2553. https://doi.org/10.1182/blood-2002-03-0819.
32. Hayflick JS, Kilgannon P, Gallatin WM. 1998. The intercellular adhesion molecule (ICAM) family of proteins. New members and novel functions. Immunol Res 17:313–327.
33. de Fougerolles AR, Stacker SA, Schwarting R, Springer TA. 1991. Characterization of ICAM-2 and evidence for a third counter-receptor for LFA-1. J Exp Med 174:253–267. https://doi.org/10.1084/jem.174.1.253.
34. Roy J, Audette M, Tremblay MJ. 2001. Intercellular adhesion molecule-1 (ICAM-1) gene expression in human T cells is regulated by phosphotyrosyl phosphatase activity. Involvement of NF-kappaB, Ets, and palindromic interferon-gamma-responsive element-binding sites. J Biol Chem 276:14553–14561.
35. Vigan R, Neil SJ. 2010. Determinants of tetherin antagonism in the transmembrane domain of the human immunodeficiency virus type 1 Vpu protein. J Virol 84:12958–12970. https://doi.org/10.1128/JVI.01699-10.
36. Garrido M, Mozos A, Martinez A, Garcia F, Serafin A, Morente V, Caballero M, Gil C, Fumero E, Miro JM, Climent N, Gatell JM, Alos L.

2007. HIV-1 upregulates intercellular adhesion molecule-1 gene expression in lymphoid tissue of patients with chronic HIV-1 infection. J Acquir Immune Defic Syndr 46:268–274. https://doi.org/10.1097/QAI.0b013e318142c74c.
37. Park SW, Royal W III, Semba RD, Wiegand GW, Griffin DE. 1998. Expression of adhesion molecules and CD28 on T lymphocytes during human immunodeficiency virus infection. Clin Diagn Lab Immunol 5:583–587.
38. Mangeat B, Gers-Huber G, Lehmann M, Zufferey M, Luban J, Piguet V. 2009. HIV-1 Vpu neutralizes the antiviral factor Tetherin/BST-2 by binding it and directing its beta-TrCP2-dependent degradation. PLoS Pathog 5:e1000574. https://doi.org/10.1371/journal.ppat.1000574.
39. Sauter D, Schindler M, Specht A, Landford WN, Munch J, Kim KA, Votteler J, Schubert U, Bibollet-Ruche F, Keele BF, Takehisa J, Ogando Y, Ochsenbauer C, Kappes JC, Ayouba A, Peeters M, Learn GH, Shaw G, Sharp PM, Bieniasz P, Hahn BH, Hatziioannou T, Kirchhoff F. 2009. Tetherin-driven adaptation of Vpu and Nef function and the evolution of pandemic and nonpandemic HIV-1 strains. Cell Host Microbe 6:409–421. https://doi.org/10.1016/j.chom.2009.10.004.
40. Scott DW, Dunn TS, Ballestas ME, Litovsky SH, Patel RP. 2013. Identification of a high-mannose ICAM-1 glycoform: effects of ICAM-1 hypoglycosylation on monocyte adhesion and outside in signaling. Am J Physiol Cell Physiol 305:C228–C237. https://doi.org/10.1152/ajpcell.00116.2013.
41. Koike J, Sagara N, Kirikoshi H, Takagi A, Miwa T, Hirai M, Katoh M. 2000. Molecular cloning and genomic structure of the betaTRCP2 gene on chromosome 5q35.1. Biochem Biophys Res Commun 269:103–109. https://doi.org/10.1006/bbrc.2000.2241.
42. Tervo HM, Homann S, Ambiel I, Fritz JV, Fackler OT, Keppler OT. 2011. beta-TrCP is dispensable for Vpu's ability to overcome the CD317/Tetherin-imposed restriction to HIV-1 release. Retrovirology 8:9. https://doi.org/10.1186/1742-4690-8-9.
43. Kueck T, Foster TL, Weinelt J, Sumner JC, Pickering S, Neil SJ. 2015. Serine phosphorylation of HIV-1 Vpu and its binding to tetherin regulates interaction with clathrin adaptors. PLoS Pathog 11:e1005141. https://doi.org/10.1371/journal.ppat.1005141.
44. Paquette JS, Fortin JF, Blanchard L, Tremblay MJ. 1998. Level of ICAM-1 surface expression on virus producer cells influences both the amount of virion-bound host ICAM-1 and human immunodeficiency virus type 1 infectivity. J Virol 72:9329–9336.
45. Beausejour Y, Tremblay MJ. 2004. Envelope glycoproteins are not required for insertion of host ICAM-1 into human immunodeficiency virus type 1 and ICAM-1-bearing viruses are still infectious despite a suboptimal level of trimeric envelope proteins. Virology 324:165–172. https://doi.org/10.1016/j.virol.2004.03.029.
46. Kondo N, Melikyan GB. 2012. Intercellular adhesion molecule 1 promotes HIV-1 attachment but not fusion to target cells. PLoS One 7:e44827. https://doi.org/10.1371/journal.pone.0044827.
47. Aguilar-Cordova E, Chinen J, Donehower L, Lewis DE, Belmont JW. 1994. A sensitive reporter cell line for HIV-1 tat activity, HIV-1 inhibitors, and T cell activation effects. AIDS Res Hum Retroviruses 10:295–301. https://doi.org/10.1089/aid.1994.10.295.
48. Derdeyn CA, Decker JM, Sfakianos JN, Wu X, O'Brien WA, Ratner L, Kappes JC, Shaw GM, Hunter E. 2000. Sensitivity of human immunodeficiency virus type 1 to the fusion inhibitor T-20 is modulated by coreceptor specificity defined by the V3 loop of gp120. J Virol 74:8358–8367. https://doi.org/10.1128/JVI.74.18.8358-8367.2000.
49. Bounou S, Giguere JF, Cantin R, Gilbert C, Imbeault M, Martin G, Tremblay MJ. 2004. The importance of virus-associated host ICAM-1 in human immunodeficiency virus type 1 dissemination depends on the cellular context. FASEB J 18:1294–1296.
50. Monks CR, Freiberg BA, Kupfer H, Sciaky N, Kupfer A. 1998. Three-dimensional segregation of supramolecular activation clusters in T cells. Nature 395:82–86. https://doi.org/10.1038/25764.
51. Zhang Z, Wu N, Lu Y, Davidson D, Colonna M, Veillette A. 2015. DNAM-1 controls NK cell activation via an ITT-like motif. J Exp Med 212:2165–2182. https://doi.org/10.1084/jem.20150792.
52. Dransfield I, Cabanas C, Barrett J, Hogg N. 1992. Interaction of leukocyte integrins with ligand is necessary but not sufficient for function. J Cell Biol 116:1527–1535. https://doi.org/10.1083/jcb.116.6.1527.
53. Haller C, Muller B, Fritz JV, Lamas-Murua M, Stolp B, Pujol FM, Keppler OT, Fackler OT. 2014. HIV-1 Nef and Vpu are functionally redundant broad-spectrum modulators of cell surface receptors, including tetraspanins. J Virol 88:14241–14257. https://doi.org/10.1128/JVI.02333-14.
54. van de Stolpe A, van der Saag PT. 1996. Intercellular adhesion molecule-1. J Mol Med 74:13–33. https://doi.org/10.1007/BF00202069.
55. Dustin ML, Springer TA. 1989. T-cell receptor cross-linking transiently stimulates adhesiveness through LFA-1. Nature 341:619–624. https://doi.org/10.1038/341619a0.
56. de Fougerolles AR, Qin X, Springer TA. 1994. Characterization of the function of intercellular adhesion molecule (ICAM)-3 and comparison with ICAM-1 and ICAM-2 in immune responses. J Exp Med 179:619–629. https://doi.org/10.1084/jem.179.2.619.
57. Bego MG, Cong L, Mack K, Kirchhoff F, Cohen EA. 2016. Differential control of BST2 restriction and plasmacytoid dendritic cell antiviral response by antagonists encoded by HIV-1 group M and O strains. J Virol 90:10236–10246. https://doi.org/10.1128/JVI.01131-16.
58. Douglas JL, Viswanathan K, McCarroll MN, Gustin JK, Fruh K, Moses AV. 2009. Vpu directs the degradation of the human immunodeficiency virus restriction factor BST-2/Tetherin via a {beta}TrCP-dependent mechanism. J Virol 83:7931–7947. https://doi.org/10.1128/JVI.00242-09.
59. Mitsuda S, Yokomichi T, Yokoigawa J, Kataoka T. 2014. Ursolic acid, a natural pentacyclic triterpenoid, inhibits intracellular trafficking of proteins and induces accumulation of intercellular adhesion molecule-1 linked to high-mannose-type glycans in the endoplasmic reticulum. FEBS Open Bio 4:229–239. https://doi.org/10.1016/j.fob.2014.02.009.
60. Bolduan S, Hubel P, Reif T, Lodermeyer V, Hohne K, Fritz JV, Sauter D, Kirchhoff F, Fackler OT, Schindler M, Schubert U. 2013. HIV-1 Vpu affects the anterograde transport and the glycosylation pattern of NTB-A. Virology 440:190–203. https://doi.org/10.1016/j.virol.2013.02.021.
61. Waheed AA, MacDonald S, Khan M, Mounts M, Swiderski M, Xu Y, Ye Y, Freed EO. 2016. The Vpu-interacting protein SGTA regulates expression of a non-glycosylated tetherin species. Sci Rep 6:24934. https://doi.org/10.1038/srep24934.
62. Banerjee P, Feuer G, Barker E. 2007. Human T-cell leukemia virus type 1 (HTLV-1) p12I down-modulates ICAM-1 and -2 and reduces adherence of natural killer cells, thereby protecting HTLV-1-infected primary $CD4^+$ T cells from autologous natural killer cell-mediated cytotoxicity despite the reduction of major histocompatibility complex class I molecules on infected cells. J Virol 81:9707–9717. https://doi.org/10.1128/JVI.00887-07.
63. Coscoy L, Ganem D. 2001. A viral protein that selectively downregulates ICAM-1 and B7-2 and modulates T cell costimulation. J Clin Invest 107:1599–1606. https://doi.org/10.1172/JCI12432.
64. Grover JR, Veatch SL, Ono A. 2015. Basic motifs target PSGL-1, CD43, and CD44 to plasma membrane sites where HIV-1 assembles. J Virol 89:454–467. https://doi.org/10.1128/JVI.02178-14.
65. Jolly C, Mitar I, Sattentau QJ. 2007. Adhesion molecule interactions facilitate human immunodeficiency virus type 1-induced virological synapse formation between T cells. J Virol 81:13916–13921. https://doi.org/10.1128/JVI.01585-07.
66. Dimitrov DS, Willey RL, Sato H, Chang LJ, Blumenthal R, Martin MA. 1993. Quantitation of human immunodeficiency virus type 1 infection kinetics. J Virol 67:2182–2190.
67. Chen P, Hubner W, Spinelli MA, Chen BK. 2007. Predominant mode of human immunodeficiency virus transfer between T cells is mediated by sustained Env-dependent neutralization-resistant virological synapses. J Virol 81:12582–12595. https://doi.org/10.1128/JVI.00381-07.
68. Galloway NL, Doitsh G, Monroe KM, Yang Z, Munoz-Arias I, Levy DN, Greene WC. 2015. Cell-to-cell transmission of HIV-1 is required to trigger pyroptotic death of lymphoid-tissue-derived CD4 T cells. Cell Rep 12:1555–1563. https://doi.org/10.1016/j.celrep.2015.08.011.
69. Jolly C, Booth NJ, Neil SJ. 2010. Cell-cell spread of human immunodeficiency virus type 1 overcomes tetherin/BST-2-mediated restriction in T cells. J Virol 84:12185–12199. https://doi.org/10.1128/JVI.01447-10.
70. Kuhl BD, Sloan RD, Donahue DA, Bar-Magen T, Liang C, Wainberg MA. 2010. Tetherin restricts direct cell-to-cell infection of HIV-1. Retrovirology 7:115. https://doi.org/10.1186/1742-4690-7-115.
71. Gummuluru S, Kinsey CM, Emerman M. 2000. An in vitro rapid-turnover assay for human immunodeficiency virus type 1 replication selects for cell-to-cell spread of virus. J Virol 74:10882–10891. https://doi.org/10.1128/JVI.74.23.10882-10891.2000.
72. Weng J, Krementsov DN, Khurana S, Roy NH, Thali M. 2009. Formation of syncytia is repressed by tetraspanins in human immunodeficiency virus type 1-producing cells. J Virol 83:7467–7474. https://doi.org/10.1128/JVI.00163-09.
73. Sato K, Aoki J, Misawa N, Daikoku E, Sano K, Tanaka Y, Koyanagi Y. 2008. Modulation of human immunodeficiency virus type 1 infectivity through

incorporation of tetraspanin proteins. J Virol 82:1021–1033. https://doi.org/10.1128/JVI.01044-07.
74. Bailey RL, Herbert JM, Khan K, Heath VL, Bicknell R, Tomlinson MG. 2011. The emerging role of tetraspanin microdomains on endothelial cells. Biochem Soc Trans 39:1667–1673. https://doi.org/10.1042/BST20110745.
75. Jolly C, Sattentau QJ. 2007. Human immunodeficiency virus type 1 assembly, budding, and cell-cell spread in T cells take place in tetraspanin-enriched plasma membrane domains. J Virol 81:7873–7884. https://doi.org/10.1128/JVI.01845-06.
76. Krementsov DN, Weng J, Lambele M, Roy NH, Thali M. 2009. Tetraspanins regulate cell-to-cell transmission of HIV-1. Retrovirology 6:64. https://doi.org/10.1186/1742-4690-6-64.
77. Arhel N, Lehmann M, Clauss K, Nienhaus GU, Piguet V, Kirchhoff F. 2009. The inability to disrupt the immunological synapse between infected human T cells and APCs distinguishes HIV-1 from most other primate lentiviruses. J Clin Invest 119:2965–2975. https://doi.org/10.1172/JCI38994.
78. Springer TA, Davignon D, Ho MK, Kurzinger K, Martz E, Sanchez-Madrid F. 1982. LFA-1 and Lyt-2,3, molecules associated with T lymphocyte-mediated killing; and Mac-1, an LFA-1 homologue associated with complement receptor function. Immunol Rev 68:171–195. https://doi.org/10.1111/j.1600-065X.1982.tb01064.x.
79. Bego MG, Cote E, Aschman N, Mercier J, Weissenhorn W, Cohen EA. 2015. Vpu exploits the cross-talk between BST2 and the ILT7 receptor to suppress anti-HIV-1 responses by plasmacytoid dendritic cells. PLoS Pathog 11:e1005024. https://doi.org/10.1371/journal.ppat.1005024.
80. Levesque K, Zhao YS, Cohen EA. 2003. Vpu exerts a positive effect on HIV-1 infectivity by down-modulating CD4 receptor molecules at the surface of HIV-1-producing cells. J Biol Chem 278:28346–28353. https://doi.org/10.1074/jbc.M300327200.
81. Cohen GB, Gandhi RT, Davis DM, Mandelboim O, Chen BK, Strominger JL, Baltimore D. 1999. The selective downregulation of class I major histocompatibility complex proteins by HIV-1 protects HIV-infected cells from NK cells. Immunity 10:661–671. https://doi.org/10.1016/S1074-7613(00)80065-5.
82. Klimkait T, Strebel K, Hoggan MD, Martin MA, Orenstein JM. 1990. The human immunodeficiency virus type 1-specific protein Vpu is required for efficient virus maturation and release. J Virol 64:621–629.
83. Binette J, Dube M, Mercier J, Halawani D, Latterich M, Cohen EA. 2007. Requirements for the selective degradation of CD4 receptor molecules by the human immunodeficiency virus type 1 Vpu protein in the endoplasmic reticulum. Retrovirology 4:75. https://doi.org/10.1186/1742-4690-4-75.
84. Gottlinger HG, Dorfman T, Cohen EA, Haseltine WA. 1993. Vpu protein of human immunodeficiency virus type 1 enhances the release of capsids produced by gag gene constructs of widely divergent retroviruses. Proc Natl Acad Sci U S A 90:7381–7385. https://doi.org/10.1073/pnas.90.15.7381.
85. Pham TN, Lukhele S, Dallaire F, Perron G, Cohen EA. 2016. Enhancing virion tethering by BST2 sensitizes productively and latently HIV-infected T cells to ADCC mediated by broadly neutralizing antibodies. Sci Rep 6:37225. https://doi.org/10.1038/srep37225.
86. Richard J, Sindhu S, Pham TN, Belzile JP, Cohen EA. 2010. HIV-1 Vpr up-regulates expression of ligands for the activating NKG2D receptor and promotes NK cell-mediated killing. Blood 115:1354–1363. https://doi.org/10.1182/blood-2009-08-237370.
87. Spenlehauer C, Gordon CA, Trkola A, Moore JP. 2001. A luciferase-reporter gene-expressing T-cell line facilitates neutralization and drug-sensitivity assays that use either R5 or X4 strains of human immunodeficiency virus type 1. Virology 280:292–300. https://doi.org/10.1006/viro.2000.0780.